

Finite Element Modelling of a High Strength Steel Tee Joint

Test Simulation



Bachelor's thesis

Visamäki, Construction Engineering

Spring, 2019

Philipp Veresov

Degree Programme in Construction Engineering
Visamäki

Author	Philipp Veresov	Year 2019
Subject	Finite Element Modelling of a High Strength Steel Tee Joint	
Supervisor(s)	Zhongcheng Ma and Jarmo Havula	

ABSTRACT

HAMK Tech (formerly known as HAMK Sheet Metal Centre) commissioned this Bachelor's thesis in continuation of a research project of high strength steel welded joints using SSAB's Strenx line of products. The goal was to create a finite element model of a tee joint test performed in the previous Bachelor's thesis of the project by Jimmy Giraldo.

The main body of the thesis describes the model creation process in LS-Dyna and LS-PrePost, decisions made along the way (especially in the definition of material properties) and mentions discarded options for future reference. Plenty of references are given to previous Bachelor's theses in the series, in order to weave them into continuing research and to provide a solid foundation for further inquiries.

The overall results of the thesis are inconclusive. The created model seems to be serving as a perfect model of tests described in *Giraldo (2018)*. However, more work will need to be done in order to reach a correlation between tests and models. A few suggestions on how to proceed further with the project are given in the conclusion.

Keywords high strength steel, heat affected zone, FE modelling, finite element modelling, LS-Dyna, LS-PrePost, magic of math.

Pages 48 pages including appendices 13 pages

A thank you note

“To make no mistakes is not in the power of a man; but from their errors and mistakes, the wise and good learn wisdom for the future.”

- Plutarch

There is no better way to start an essay than to appropriate a piece of wisdom from someone smarter than you are.

My studies in HAMK and work in Ohutlevykeskus have been tough and rewarding. The daily toil of learning was (and still is) a significant part of my life. I have made many mistakes along the way. But hopefully this last hooray of my Bachelor's degree will help to cultivate future good work.

With that, I would like to thank my thesis supervisors, Jarmo Havula and Zhongcheng Ma, for their patient guidance and ingenuity with providing me with a challenging yet manageable thesis topic. I had to learn a great deal more about engineering in order to complete this work, learning more about finite element modelling than any average bachelor level student of engineering. I am deeply grateful for that opportunity.

In addition, I would like to mention a few of the teachers and staff members from my degree program, whose advice and support was instrumental in my journey towards a degree: Cristina Tirteu, Tapio Korkeamäki, Anu Virtanen, Helena Parviainen and Jani Tolvanen.

Likewise, my friends deserve a mention too. Vu Pham Nguyen for being an inspiration to power through the mundanity of learning and achieving a better understanding of structural engineering. Semion Iudin for constant help with writing advice and reading my early drafts. Irina Gladkikh for moral support. Natacha Buntinx for complimenting my writing style and encouraging me to write more flamboyantly than I would otherwise do. Ronjit Medda for igniting my interest in technical writing. Lev Chumichev for being a good source of quotes. Elizaveta Grigoreva for the music support. Zoey for being the best girl. However, there are so many of, that I can write a whole book of gratitude, therefore big hugs and thank you - see you at the party!

Last, but not least, a thank you to my family for supporting me in my endeavors.

Philipp Veresov

Visamäki, 13th of March 2019

CONTENTS

1	INTRODUCTION	1
1.1	Research question	1
1.2	Background.....	1
1.2.1	Weld run tests	2
1.2.2	Tee joint tests	2
1.2.3	The big research project	3
1.2.4	A note on tubular members	4
2	TRANSFORMATION OF PARAMETERS INTO LS-DYNA	4
2.1	Choice of the specimen from <i>Giraldo (2018)</i>	4
2.2	Modelling the geometry.....	9
2.2.1	General dimensions of the specimen and the model	9
2.2.2	Regions of the model.....	13
2.2.3	Choice of the element type	14
2.3	Modelling of the materials	16
2.3.1	Strenx 700MC transformation.....	17
2.3.2	Filler material transformation	21
2.3.3	Heat-affected zone transformation	25
2.4	Load, support conditions and load path	33
2.4.1	Load application in LS-Dyna.....	33
2.4.2	Support conditions	36
2.5	Final model geometry and hardware limitations.....	37
3	ANALYSIS OF THE SIMULATION OF IMPROVED MODEL.....	38
4	CONCLUSION	44
5	RECOMMENDATIONS AND FUTURE WORK.....	44
5.1.1	On the modelling side.....	44
5.1.2	On the testing side.....	45
5.1.3	Organizational suggestions.....	45
	REFERENCES.....	46
	INTERVIEWS.....	48
	Appendices.....	49
	Appendix 1 Modelling order	
	Appendix 2 Problem of elongation measurement	
	Appendix 3 Methodology of Engineering to True	
	Appendix 4 Devised options for weld/HAZ balance	
	Appendix 5 MAT024 input	
	Appendix 6 About heat input	
	Appendix 7 Some sources for self-tutelage in LS-Dyna	

1 INTRODUCTION

1.1 Research question

The goal of this thesis is to create a FE model based on the test results presented by *Giraldo (2018)*, in order to check if a reliable mathematical model of the tests can be created. Other Bachelor's theses (*Nguyen (2018)*, *Grecevcic (2016)* and *Abebe (2016)*) are used to verify the results obtained by *Giraldo (2018)* in his study. To achieve this goal, a few material and geometrical models of the tee-joint will be created with the help of experienced LsDyna user and professor in HAMK Zhongcheng Ma as well as with extensive use of online guides.

1.2 Background

The Bachelor's thesis you are currently reading is part of a research project about welding of high-strength steel (specifically SSAB HSS Strenx product). This research project is a long-term research into application of tubular steel structures, which by design constraints of the material, requires a lot of welding to service the structural models used in their design. Welding of steel is a complex business by itself, but it has been extensively researched over the last century and now it is time to extend traditional boundaries of the craft with research of welding of high strength steel.

While normal structural steel requires sufficient fusion and matching materials for a weld to be effective, high strength steel needs additional restrictions. For example, Strenx is a tempered high strength steel, meaning it undergoes a rapid cooling process, cementing an atomic structure of a steel at a higher temperature, which otherwise cannot exist at ambient temperature, making this alloy temperature sensitive.

Therefore, when welding is performed, the temperature has to rise above steel melting point and then to cool off. While it happens, steel atomic structure undergoes a change, too, akin to baking. With normal steel, cooling time to ambient temperature is not a problem, it simply needs to be long enough to ensure that fusion of two parts and of the welding material is complete. With high strength steels though, there is a constraint of too long cooling time, which will normalize high strength steel down to normal steel, making the weld a critical part of the joint, which is outside of the ultimate limit state design philosophy of the Eurocode (*EN 1990*).

1.2.1 Weld run tests

Cooling time can be controlled by applying different welding procedures, which usually ends up in a different number of weld runs needed to be performed, in order to reduce the cooling time of each run and subsequently the "baking time" of the entire weld. Previous bachelor level researches in this project were aimed at this problem (specifically *Nguyen (2018)* and *Grecevci (2016)*). Both ran similar test programs to determine the influence of different number of weld runs on the ultimate tensile strength of different Strenx grades (from 420 to 960). In both studies, cooling time and heat input were measured and used as quality control parameters, which are later used in the definition of welding procedures. However, practical guide to efficiency of different number of weld runs were based on tensile tests, results of which were varied and far between.

Unfortunately, despite the best efforts of Nguyen and Grecevci, exact reasons for the variety in results of tensile tests of similar Strenx grades were not individualized, even though both authors have suggested a few possible causes of it. Those causes include unevenness of the welding process itself, poor surface preparation prior to welding, incorrect choice of the filler material and a few others issues. For the purpose of this thesis, it is important to state that such variety of uncertainties in the properties of the weld is a hiccup. If you want to know more about the discussion, check *Nguyen (2018)* and *Grecevci (2016)*.

The problem with notions of cooling time and heat input is that ultimately the basic unit of energy input into welding is the same, so the joint will be weaker overall. The process of electric arc welding used in the tests requires a basic unit of energy input to achieve the melting point across any number of welds, leaving cooling time as primary quality control parameter of welding quality of high strength steel. This creates a challenge with implementation of cooling time results in the design of welded joints, since the basic principle of structural safety requires welds to be the strongest part of the joint, because "baking" nature of the cooling process of welds leaves uncertainties in its final properties (especially in ductility, affecting rotational capacity of the joint).

1.2.2 Tee joint tests

Girlando and Abebe wrote two more Bachelor's theses for this project. With a goal of covering direct tests of tubular T-joints, with an emphasis on resistance of welds, working towards a direct application and possible modifications of existing tubular joint design procedures.

In *Abebe (2016)*, full-scale tubular joint specimens were manufactured, yet due to financial restraints full-scale tests were not performed, retreating to smaller, but mechanically similar specimens. Unfortunately, despite smart solutions to enforce necessary force distribution, specimen

manufacturing proved to be too complex and convoluted, resulting in yet more uncertainties in test results.

In *Giraldo's study (2018)*, manufacturing process and load arrangement were simplified, which was supposed to yield more predictable and reliable results. However, despite the best efforts of all contributors, problems with weld properties and procedures similar to *Nguyen (2018)*, *Grecevcic (2016)* and *Abebe (2016)* as well as new challenges in displacement verification caused by permanent deformation of the "testing jig", resulting in highly varied test results.

Further discussion on the usage of previous test results in material and geometry modelling is discussed in the relevant parts of the thesis.

1.2.3 The big research project

The big research project is about a wider application of global plastic analysis with semi-rigid joints. The task is to provide more precise rules for estimation of initial in-plane rotational stiffness of welded tubular joints and to apply those rules to both structural and high strength steels. It might seem that the scope of the project is quite limited, yet welded tubular joints are the basis of modern steel structures (e.g. prefabricated roof systems, specifically trusses).

The challenge is that normally elastic global analysis with either nominally pinned or rigid joints is used (allowing either full transfer of moments or none from member to member). It is a rough approximation, which greatly affects manufacturing price of joints. Naturally, most joints are neither pinned nor rigid, but semi-rigid.

Semi-rigid joints are modelled as springs, which means that their response is force related, usually measured in kNm/rad. Analysis of such response is complex, rooted in predictability and uniformity of material properties and execution techniques. Steel is a perfect material for that. Its properties are well researched and manufacturing is strictly controlled. As for execution techniques, for structural steel it is not a problem (it is well researched); however, HSS is a different matter. High strength steels are produced, using more sophisticated casting techniques (e.g. rapid tempering in case of Strenx), which make those steels harder to weld. Thus, a new welding procedure (or procedures) need to be developed and tested, in order for predictable results to be obtained from welding of those joints.

Therefore, with better welding techniques and steel with higher yield limit and better plastic properties, structural engineers will be able to design safer and cheaper steel frames. This is the ultimate goal of any engineering research and practice.

1.2.4 A note on tubular members

Tubular sections have closed type sections and classic I-sections are open sections. While I-sections are lighter when compared to tubular sections - tubular sections have better resistance parameters (e.g. in torsion caused buckling modes), which not necessarily makes them cheaper. Nevertheless, it definitely reduces required detailing needed to ensure member stability, allowing simpler secondary steelwork to be designed (EN 1993-1-1).

2 TRANSFORMATION OF PARAMETERS INTO LS-DYNA

"We are building something here detective. We are building it from scratch. All the pieces matter." - Lester Freamon from "The Wire".

In this section, transformation of parameters from the results of *Giraldo (2018)* to a finite element model of LsDyna format is presented. A simplified modelling process graph can be found in Appendix 1.

A group of related concepts gives the description of the modelling process, but the actual process is more arbitrary. Firstly, reasoning for choice of a single specimen from *Giraldo (2018)* is given and thus a choice of criteria for judgment of modelling efforts. Then the creation of the overall geometry, regions and elements of the model are described. This is followed by the definition of material model and associated material properties. The chapter is finished with a definition of load application and support conditions of the model.

2.1 Choice of the specimen from *Giraldo (2018)*

"Wind is basically air." - Confucius

At the beginning of the thesis process, a single exemplary specimen from tested specimens needed to be chosen from *Giraldo (2018)*. The tested specimens can be divided into two major groups - butt and fillet welds.

Both fillet and butt joints were manufactured of Strenx 700MC, the same filler material (OK ARISTOROD 69), in the same place (Tavastia ammattikoulu) and by the same welder (Harri Nieminen). Despite those similarities, test results vary greatly between each other.

In order to select a single specimen for modelling, the following criteria were used:

- Uniformity of failure pattern
- Presence of test results

- Ease of modelling, analysis and evaluation

Out of twelve specimens manufactured for *Giraldo (2018)*, eleven were tested. Five were butt welds of 8mm and six fillet weld specimens (two 6mm, two 10mm and two 12mm).

Note that nomenclature of specimens used in this thesis is different from the one in *Giraldo (2018)*. It is because in Giraldo's tests were divided into two batches and naming of specimens did not always correlate with the naming in Excel files with tensile test results.

Comparisons in the following Figures 1,2 and 3 are based on uniformity of the weld and its failure pattern as well as availability and reliability of load-displacement functions derived from tensile tests of *Giraldo (2018)*. Geometry of the weld itself is not considered as a critical factor in this stage of the choice, since either butt or fillet weld can be modelled with relative ease.

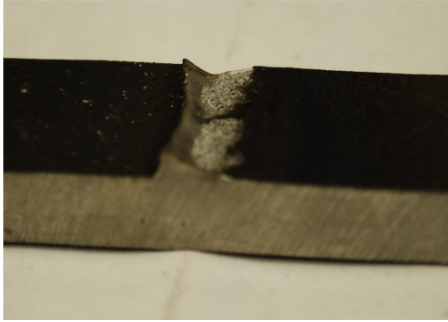
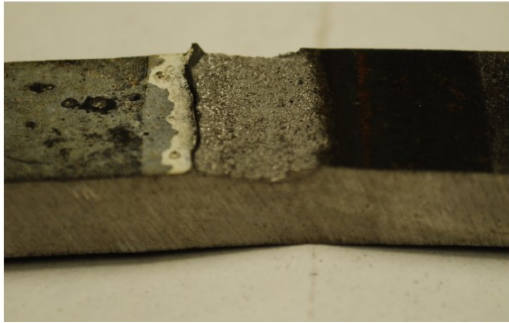
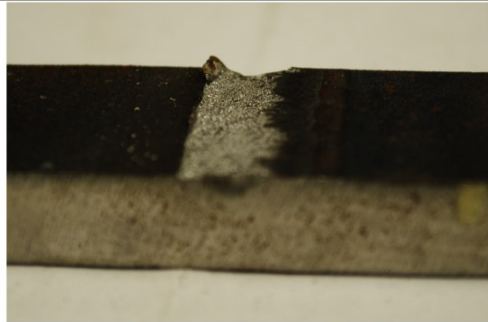


	B8_2 No results available
	B8_3 F = 57,15 kN 372 MPa ~4 mm 1 weld run
	B8_4 No results available
	B8_5 F = 74 kN 483 MPa ~6mm 1 weld run
	B8_6 No results available

Figure 1. Butt weld failures of *Giraldo (2018)*

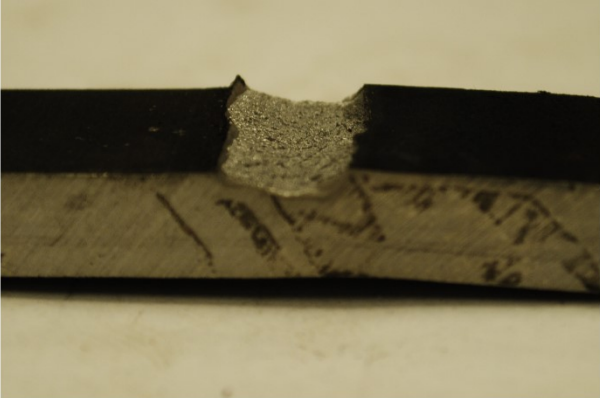
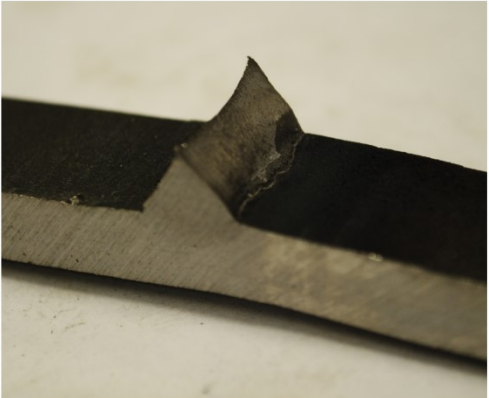
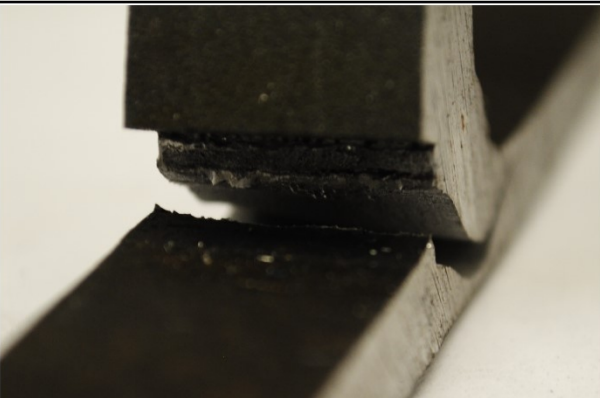
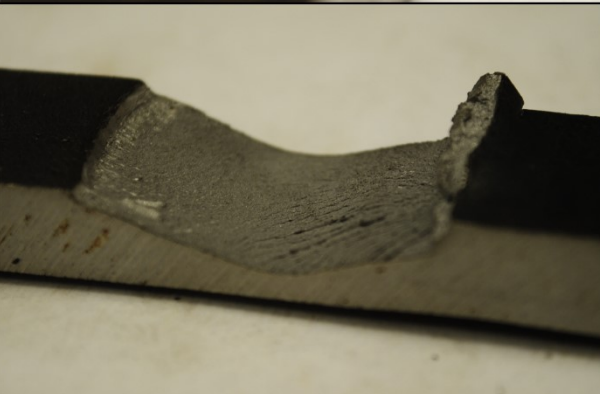
	<p>F6_1 F = 71 kN 467 MPa* 6,6 mm 1 weld run</p>
	<p>F6_2 F = 63,5 kN 418 MPa* ~8,5 mm 1 weld run</p>
	<p>F10_1 F = 46,4 kN 305 MPa ~4 mm 3 weld runs</p>
	<p>F10_2 F = 52 kN 344 MPa ~3,8 or 20 mm* 3 weld runs</p>

Figure 2. Fillet weld failures of *Giraldo (2018)* - 1

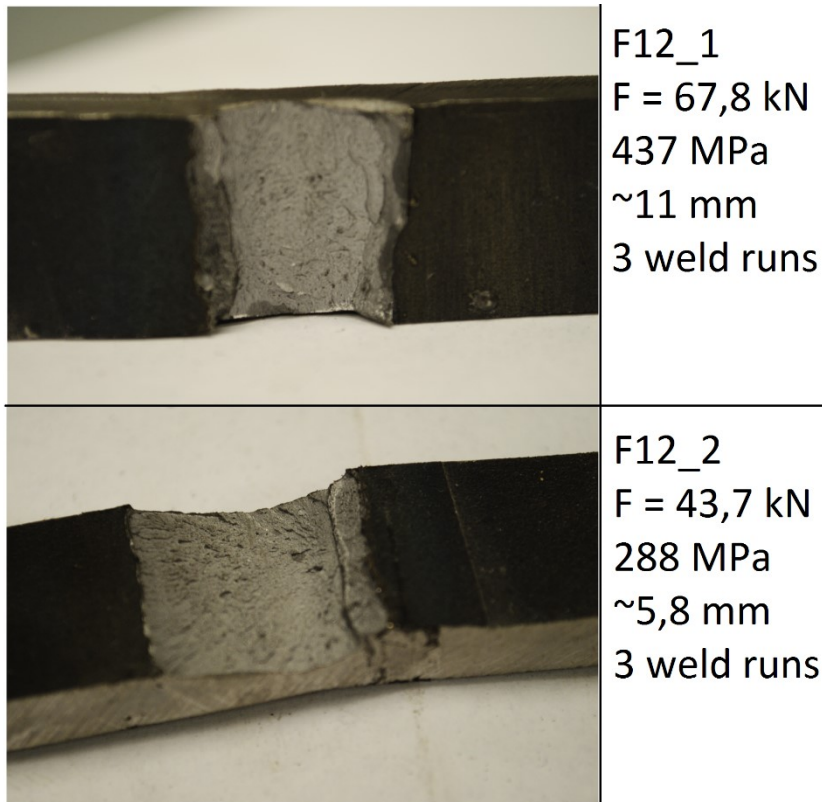


Figure 3. Fillet weld failures of *Giraldo (2018) - 2*

Regarding asterisk in stress results for F6 welds: It is marked so, because fillet weld of 6mm area is not enough to uniformly transfer stresses from a welded part with 8mm of thickness, creating a stress concentration.

In the results for butt welds, only two graphs are available from a set of five tested specimens. Even though the two specimens should be nearly identical - there is a difference in strength of 23% and difference in elongation of 34%.

In the results for fillet welds, all load-displacement graphs are available. But there is an uncertainty with their allocation to respective tested specimens. The one identified with certainty is F6_1, because the author of this thesis was assisting Giraldo in the last test series.

In case of F10_1 and F10_2 specimens, the results seem to be closer together (except for a bump in elongation in F10_2, but it can be safely disregarded due to bigger problems with elongation measurement itself). However, the failure mode is far less predictable, due to the lamellar nature of it and the multiplicity of weld runs, which complicates HAZ formation region and properties assumptions. Also, three weld runs per joint have a difference in results between lap joints (see *Nguyen (2018)* and *Grecevci (2016)*), where more weld runs per joint showed an increase in overall joint strength. While in tee joint tests (see *Abebe (2016)* and *Giraldo (2018)*), specimens with more weld runs showed worse results.

Table 1. Comparison of available results from *Giraldo (2018)*

	Failure force, kN	Difference		Failure force, kN	Difference
F6_1	71	10,56%	F12_1	67,8	35,55%
F6_2	63,5		F12_2	43,7	
F10_1	46,4	10,77%	B8_3	57,15	22,77%
F10_2	52		B8_5	74	

Specimens with fillet weld leg of 12 mm suffer from similar problems as F10 for similar reasons.

It is likely that lower resistance of theoretically stronger welds is caused by either smaller penetration of the weld into the root of the weld or by increased susceptibility to effects of the joint eccentricity by F10 and F12 compared to F6 specimens. Or both, as can be deduced from information presented in Table 1.

Therefore, for the sake of simplicity and relative predictability of design, analysis and evaluation of specimen F6_1 was chosen as a design model, especially in connection with heat input. Single weld run makes HAZ region easier to predict.

2.2 Modelling the geometry

2.2.1 General dimensions of the specimen and the model

Figure 4 shows the dimensions of specimens in *Giraldo (2018)*, even though the specific specimen was not tested (note double side fillet weld).

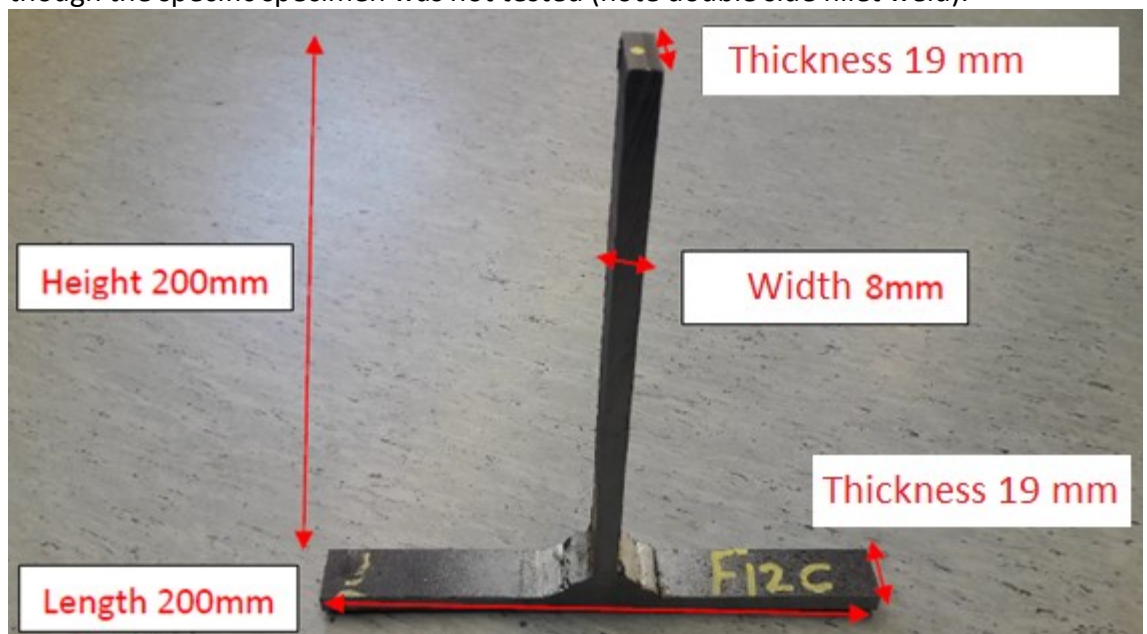


Figure 4. Specimen size (taken from *Giraldo, (2018)*)

Despite the simplicity of those dimensions, a specific leg size of the fillet weld used for the model is not 6 millimeters, as expected from the definition of a fillet weld. Instead, it is 9 millimeters, as can be seen in Figure 5, showing the bottom plate of F6_1 after failure.

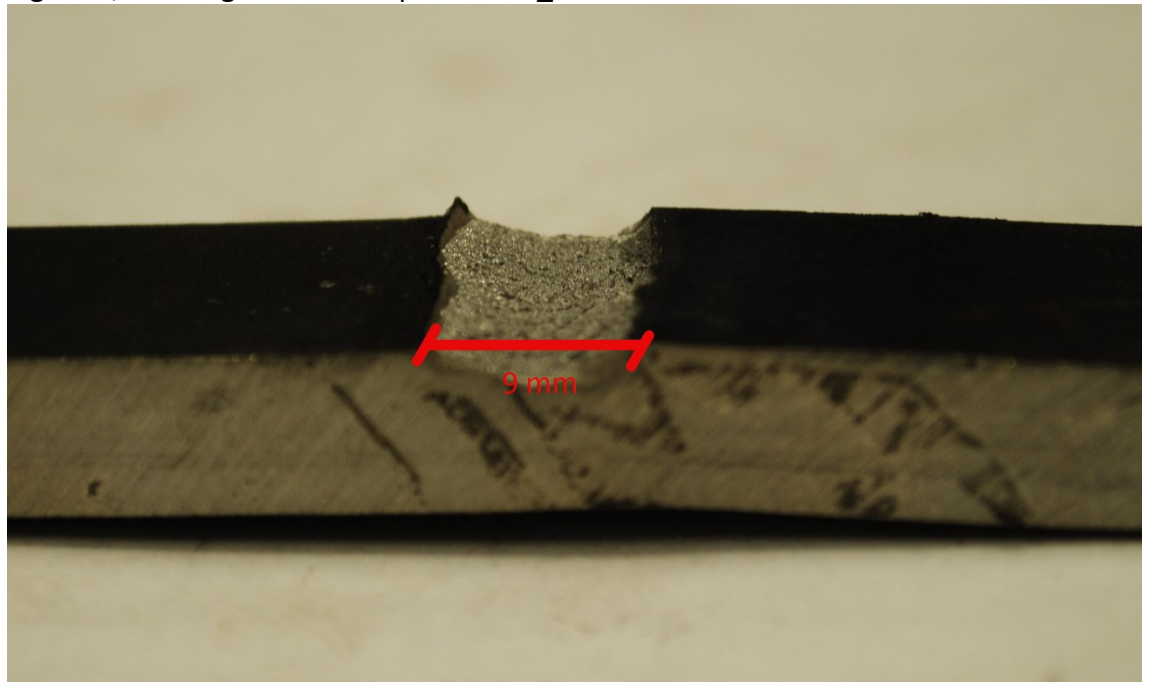


Figure 5. Failure length at the bottom plate

In addition, the real thickness of the specimen is about 19 millimeters, due to cutting issues. However, thickness measurements are used in the definition of elements only - the model is drawn in 2D mode.

Figures 6 and 7 show the definition of the general dimensions of the specimen in LS-PrePost (V4.5.22 - 13Jul2018), which is the software for the preparation and analysis of models for LS-Dyna (which is a calculator only). The dimensions were input in a 2D mode for the sake of simplicity.

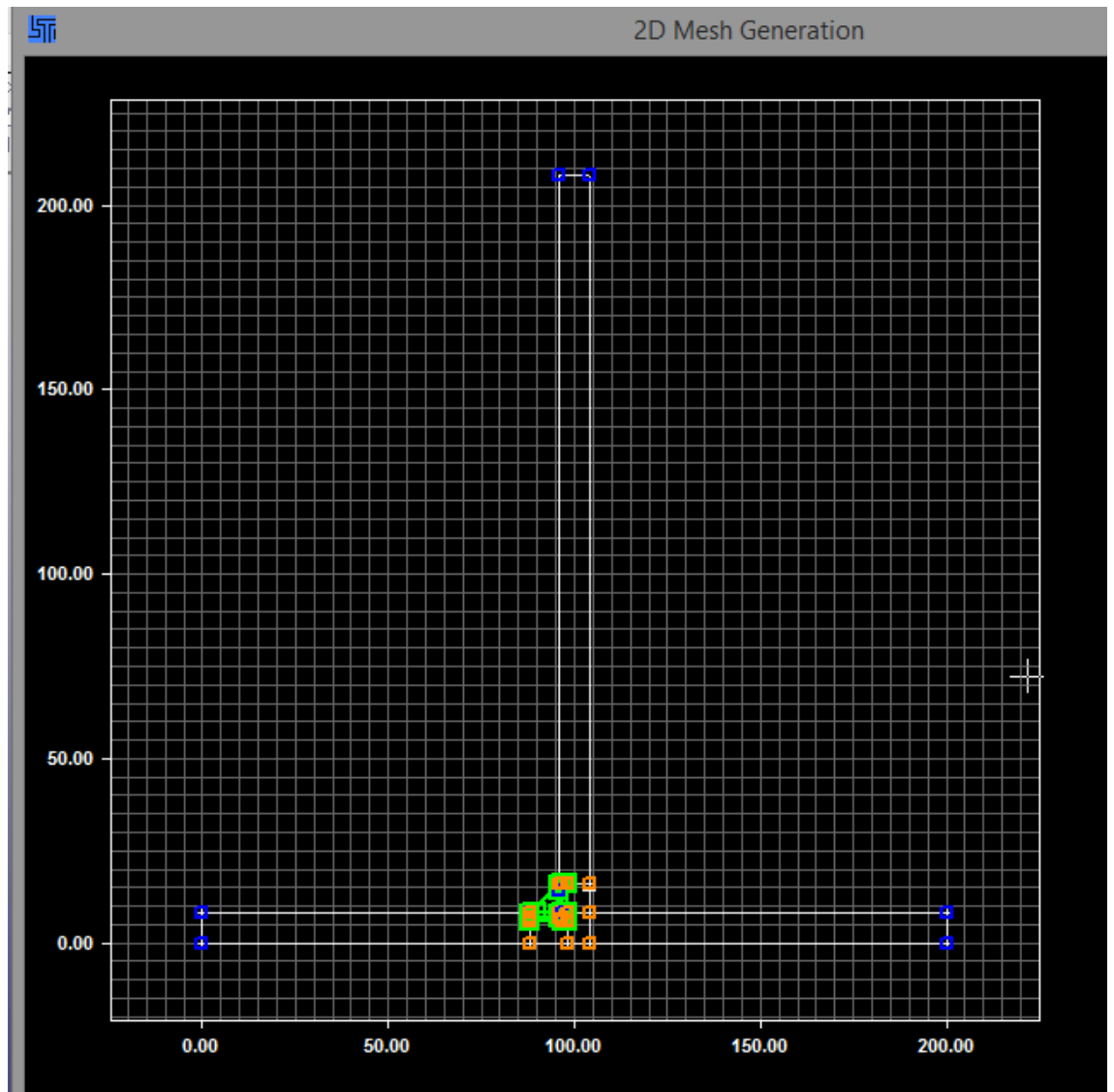


Figure 6. 2D sketch input in LS-PrePost

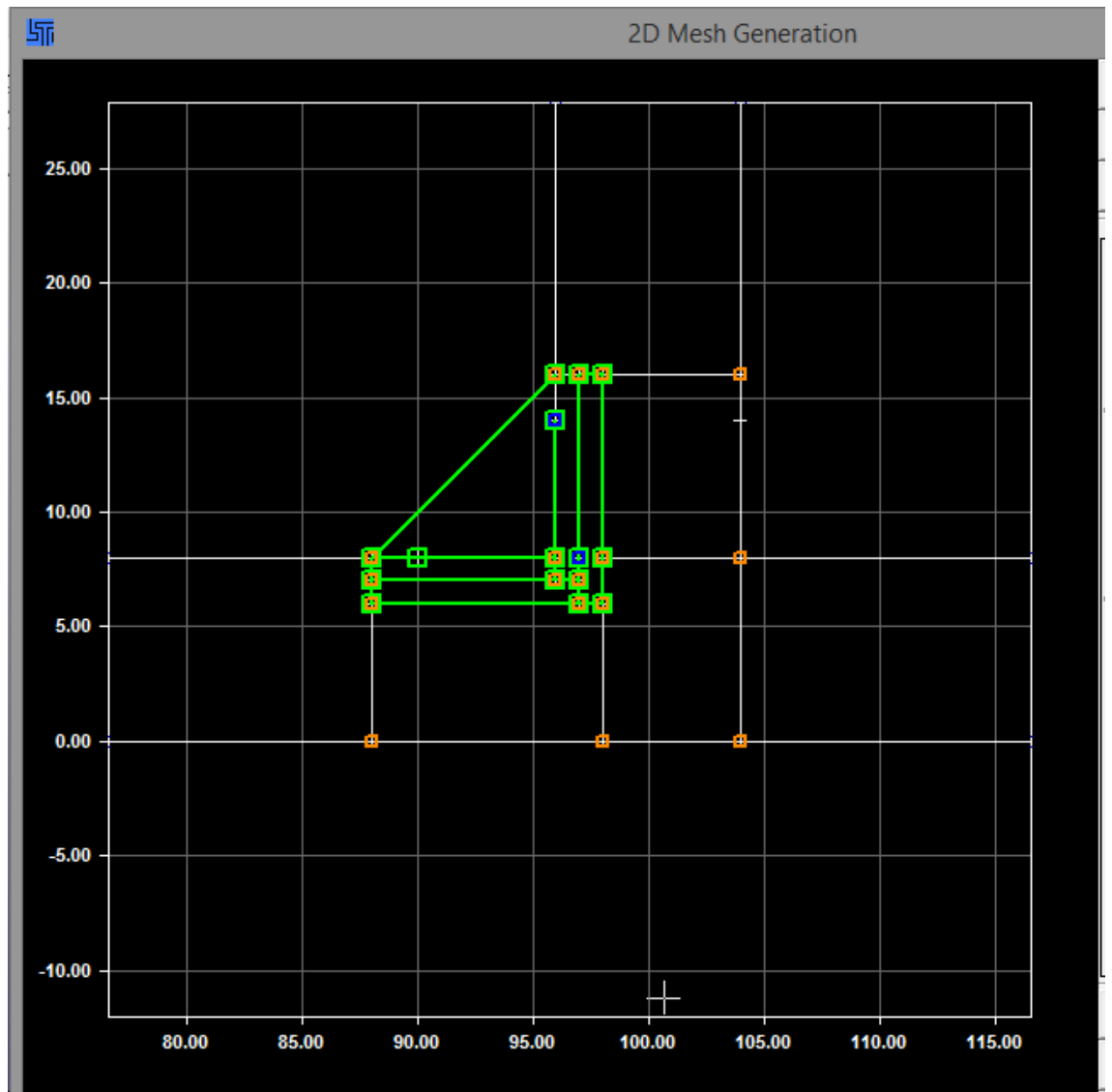


Figure 7. 2D sketch input in LS-PrePost with zoom on weld area

After the creation of node-by-node and line-by-line general boundaries of the model and its regions (parent material, heat affected zone and weld material) - see Figure 7 - it is time to subdivide individual parts into meshes by defining the number of elements per edge. This is a critical parameter for calculation time of the model and quality of the simulation. For this thesis, element size of 1 mm was used for exploratory models and 0.2 mm was used for final models, in order to achieve a better representation of stress and strain in the model.

2.2.2 Regions of the model

In this chapter, regions of the model are explained in the necessary depth and detail required for understanding of the results of this thesis. Figure 8 shows the general division of the mesh used on the specimen.

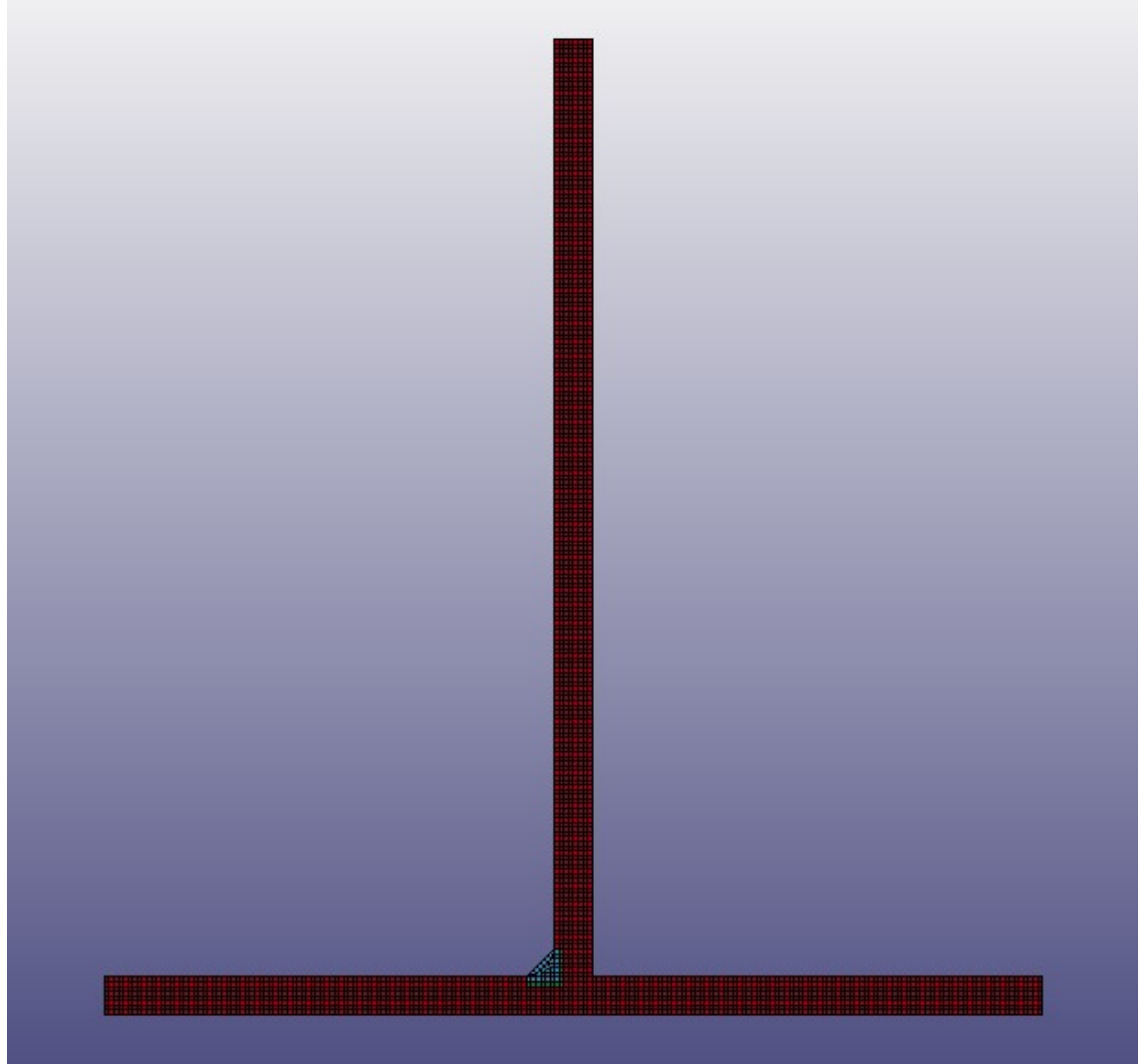


Figure 8. Result of the geometry modelling with 1mm element size

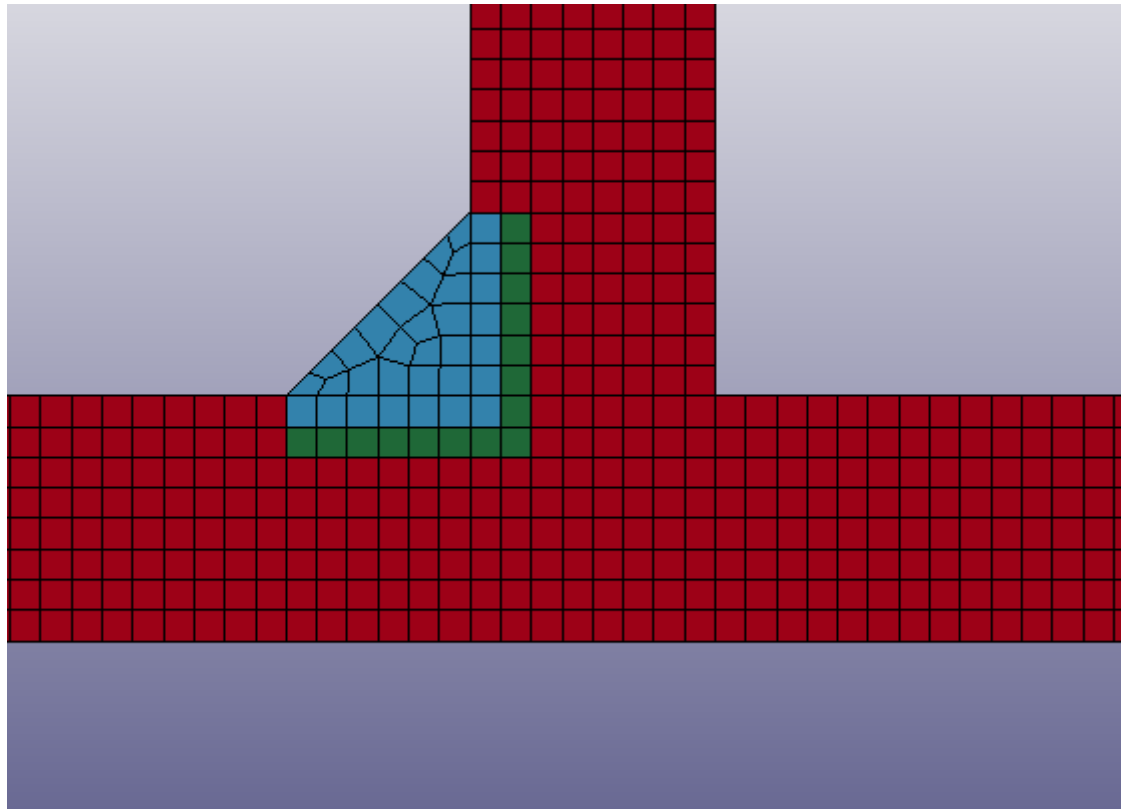


Figure 9. Results of the geometry modelling of the weld region with 1mm element size

Red mesh constitutes part designated for parent material, green for heat-affected zone (HAZ) and light blue for weld region. One-millimeter penetration of the weld zone was chosen based on a scientific approximation of the concept of weld fusion and therefore a mixing of the materials, transferring formidable (thermally stable) properties of the weld material inwards. This leaves a critical, 1mm deep region of heat-affected zone (also called baking zone) with reduced properties. Naturally, it should be more radial and dependent on the welding position, but such details are beyond the scope of this bachelors' thesis.

Meshing of regions/parts was performed automatically after defining the number of elements per edge. A less orthogonal shape of mesh in the weld region does not matter for this model, since critical zones are located at the upper part of the top leg and at the root of the weld respectively.

2.2.3 Choice of the element type

With 2D created boundary outline, a further decision has to be made - keep the model a 2D, made of shell elements, or a 3D, with detailed simulation of stress strain in all directions.

The decision between a 2D and a 3D model is a matter of available hardware capacity. A model made of 3D elements would yield an

overwhelmingly more realistic picture of the stress and strain distribution throughout the model, yet additional dimension to consider and additional elements in the thickness direction of the model would require a significant calculation time and processing power of available hardware. Naturally, both processing power and calculation time are restricted. Due to Helpdesk policies developed in HAMK, all computers are available for about 14 hours a day, with a forced hibernation of PCs starting at about 11 pm. This restriction along with only four CPUs of about 2.4 GHz limits the application of 3D elements to the level of impossibility.

Therefore, 2D elements are the only option in this particular case. Despite their seeming limitations, since shell elements create a contour of the member, working with its surfaces only - it is perfectly suited for the use in this model. Because the specimens of *Giraldo (2018)* are relatively thin in regard to its height and width (the primary dimensions), the stress and strain distribution can be assumed to be uniform. In addition, there are no external forces present in perpendicular direction. Those two factors support the adoption of 2D elements for this model without a sacrifice to the quality of the resulting force distribution.

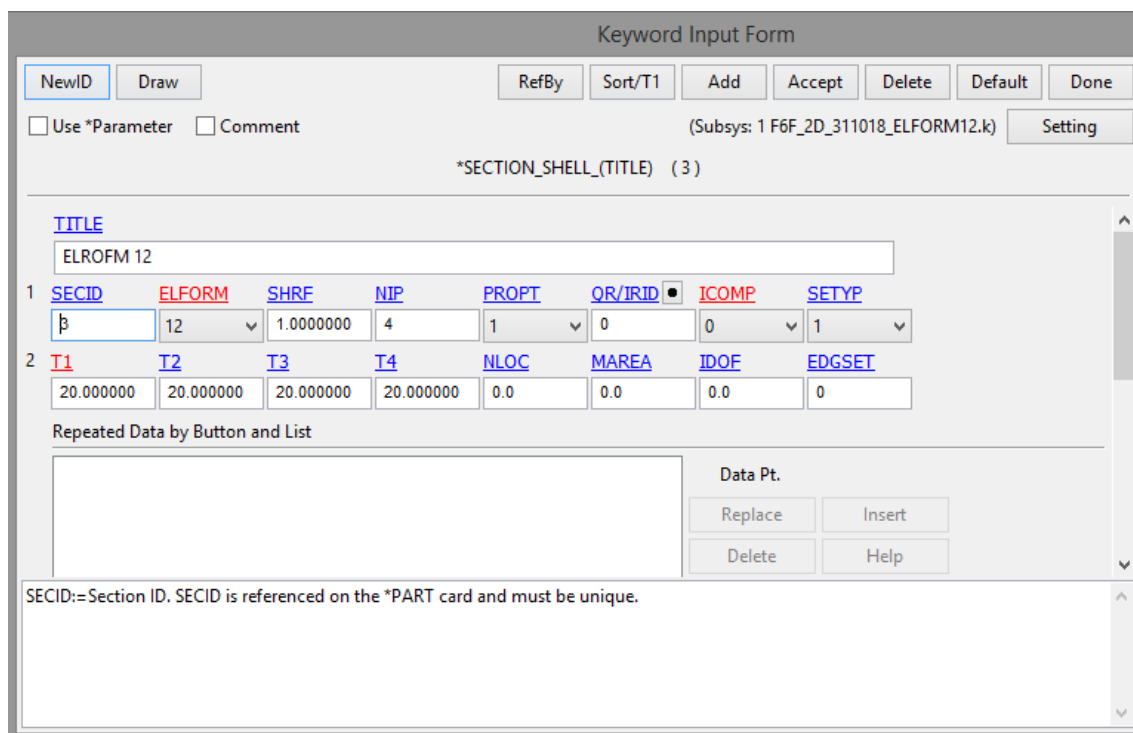
Then a decision of which of about 40 available shell element formulation options can be chosen for the model has to be made. After a discussion with thesis supervisor (*meeting on 04.09.2018*), three possible formulations were indicated: ELFORM 2, ELFROM 12 and ELFORM 13.

ELFORM 2 was neglected outright, due to its longer calculation time, which was caused by its additional considerations of perpendicular forces, making up for the lack of a third dimension. In case of the current tee joint model, such considerations are wasteful.

ELFORM 12 and ELFORM 13 are mostly similar element formulations, with the primary difference being consideration of stress to be uniform throughout thickness and strain to be uniform throughout thickness respectively. (*Digital Engineering and LS-Dyna Manual Volume 1*)

The decision was made in favor of ELFORM 12 (plane stress) shell formulation, because the problem ideally fits the framework of a plane stress model – equal stress distribution in a thickness direction.

The shell formulation option used are shown in Figure 10.



Keyword Input Form

NewID Draw RefBy Sort/T1 Add Accept Delete Default Done

Use *Parameter Comment (Subsys: 1 F6F_2D_311018_ELFORM12.k) Setting

*SECTION_SHELL_(TITLE) (3)

TITLE
ELROFM 12

1	SECID	ELFORM	SHRE	NIP	PROPT	OR/IRID	ICOMP	SETYP
	β	12	1.0000000	4	1	0	0	1
2	T1	T2	T3	T4	NLOC	MAREA	IDOF	EDGSET
	20.000000	20.000000	20.000000	20.000000	0.0	0.0	0.0	0

Repeated Data by Button and List

Data Pt.
Replace Insert
Delete Help

SECID:=Section ID. SECID is referenced on the *PART card and must be unique.

Figure 10. ELFORM 12 - Plain stress - shell formulation

Given thickness (T1-T4) is needed for the determination of the stress values for the animation of the simulation.

2.3 Modelling of the materials

“Erecting a diploma” - Вождь

This chapter covers the determination of material properties of the model. This process consists of transformation of engineering values of stress and strain of the material into true stress and strain, which is used in LS-Dyna. Methodology of transformation can be found in Appendix 3.

Strenx 700MC (parent material) and OK ARISTOROD 69 (weld or filler material) have well researched homogeneous properties and thus are defined with ease. Unlike heat-affected zone, whose depth of penetration as well as range of stress reduction (due to varying cooling time) are subject to speculation. Therefore, an assumption of homogeneity and uniformity of its properties is made outright.

To begin with, the material model has to be chosen. LS-Dyna has a variety of options (*LS-Dyna user’s manual volume 2*) available; almost 300 options to be precise. However, in the process of preliminary design (*meetings on 01.05 and 04.09.2018*) MAT024 was designated as a material model for this thesis. It is commonly used to simulate plastic and isotropic material

behavior with the definition of failure parameters, which is exactly what this model needs.

2.3.1 Strenx 700MC transformation

Usually material properties of steel are based on common knowledge, as in case of structural steel, and manufacturer's catalogue. For tests of specific batches of steel, manufacturers perform tensile and ladle tests in order to certify conformity of the delivered material to the relevant standards (e.g EN 10025-2, EN 10025-6 and EN 10049-2).

In this case, we do not have delivery note available and Strenx 700MC, which while conforming to technical delivery requirements has a few uncertainties in its properties. As can be seen in figure 11, ultimate stress varies greatly and failure strain is at the level of about 12%.

Dimension Range

Strenx 700 MC is available in thicknesses of 2.00-10.00 mm and widths up to 1600 mm as coils, slit coils or cut to length sheets in lengths up to 16 meters.

Mechanical Properties

Thickness (mm)	Yield strength R_{eH} ¹⁾²⁾ (min MPa)	Tensile strength R_m (MPa)	Elongation A_{80} ⁴⁾ (min %)	Elongation A_5 (min %)	Min. inner bending radius for a 90° bend ³⁾
2- 3	700	750- 950	10	12 ⁵⁾	0.8 x t
3.01- 6	700	750- 950		12	1.2 x t
6.01- 10	700	750- 950		12	1.6 x t

The mechanical properties are tested in the longitudinal direction.

¹⁾ If ReH is not applicable then Rp 0,2 is used.

²⁾ On thicknesses >8 mm the minimum yield strength may be 20MPa lower.

³⁾ For both longitudinal and transverse direction.

⁴⁾ A_{80} value applies for sheet thickness < 3.00 mm

⁵⁾ A_5 value applies for sheet thickness $t \geq 3$ mm.

Figure 11. SSAB Data Sheet (SSAB Datasheet for Strenx 700MC)

Therefore, ultimate tensile stress varies between 750 and 950 N/mm², which is a significant difference of 200 N/mm². There are two datasets available, which can help to make a decision:

1. Result of tensile test performed for *Grecievci (2016)* shown in Figure 12.
2. Approximation made in *Nguyen (2018)* based on hardness of the parent material

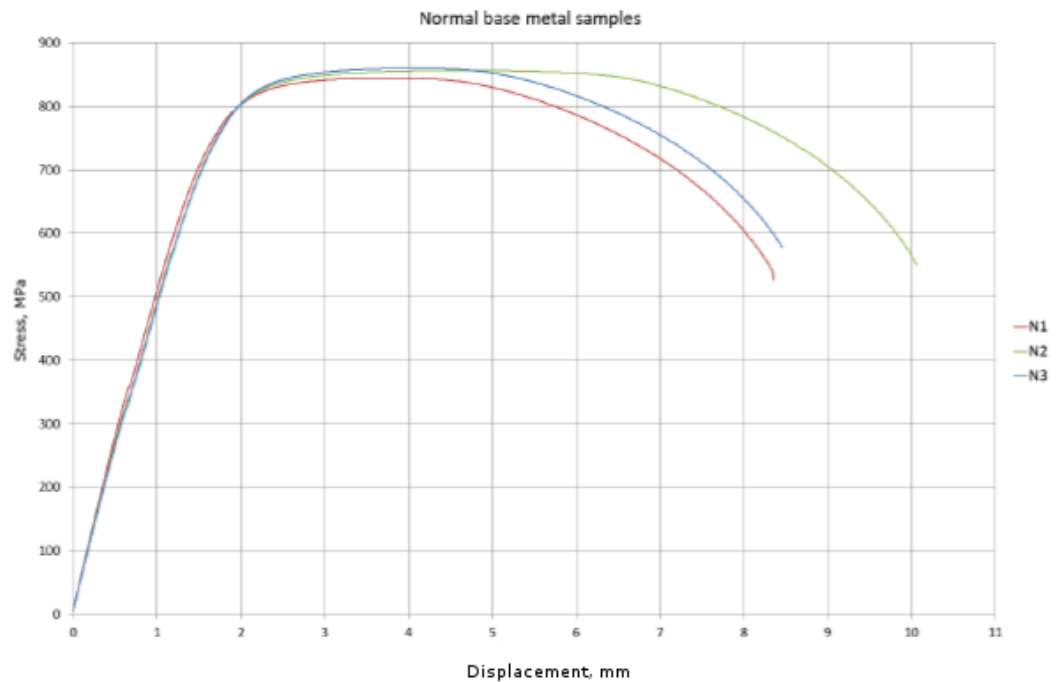


Figure 12. Results of Strenx 700 from (*Grecevci, 2016*)

Grecevci (2016) gives a value of about 850 N/mm². Strain measurement has similar problem to results of *Giraldo (2018)*. See Appendix 2 for more information about the strain.

Nguyen (2018) defines ultimate tensile stress of Strenx 700MC at about 870 N/mm², using hardness to ultimate tensile stress conversion tables. It is important to note that the results of such conversion are approximate, but in given circumstances there is no better option.

In this thesis, a compromise value of ultimate tensile stress of 860 N/mm² is adopted.

As for strain values, based on the discussion with the thesis supervisor on 04.09.2018, it was mentioned that the real failure strain of hot rolled steel can be up to 45%, when elongation is only 15-25%.

In this case, failure strain of 17% was chosen, since it is a value of failure strain of the filler material and at the same time a compromise value between the minimum elongation 12% stated in Strenx 700MC datasheet and absolute failure strain value of carbon steel of 45%.

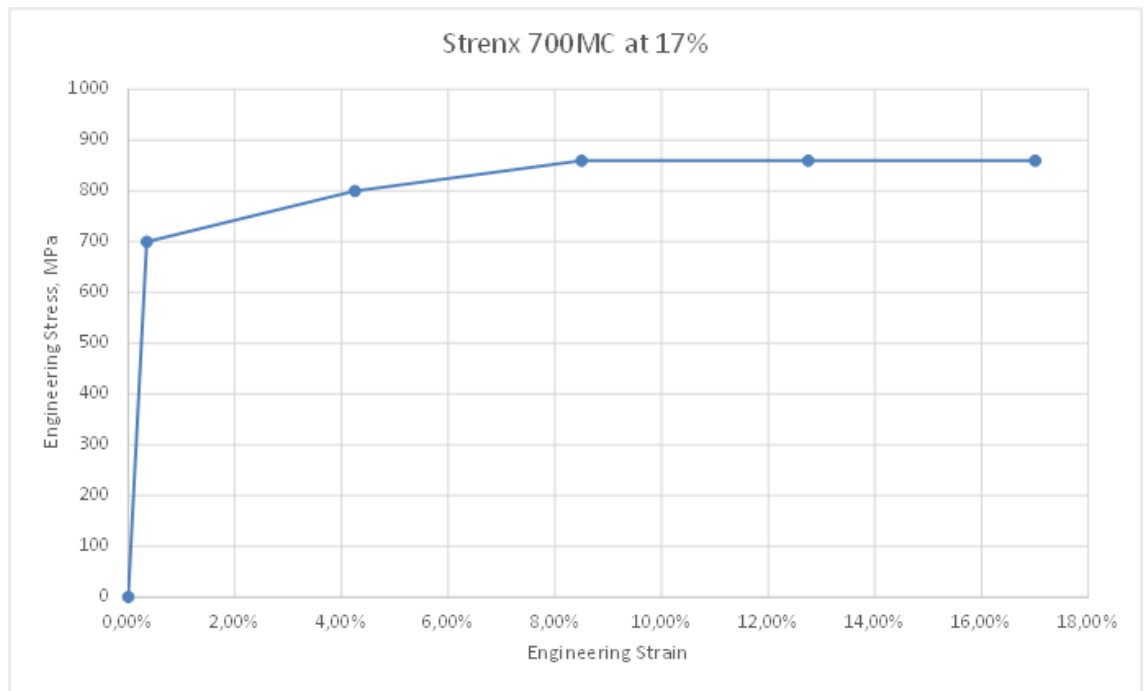


Figure 13. Engineering stress-strain curve of Strenx 700MC

Curve in Figure 13 was constructed in Excel, based on the parameters shown in Table 2:

Table 2. Input parameters for the curve in Figure 13

	MPa
Eng. Strain	Eng. Stress
0,00%	0
0,35%	700
4,25%	800
8,50%	860
12,75%	860
17,00%	860

Where yield strain is calculated based on the known yield stress of Strenx 700MC (700 MPa) and modulus of elasticity (200 GPa), using the following equation:

$$\varepsilon_{elastic} = \sigma_{yield}/E \quad (1)$$

Plastic region of the curve is based on an equal distribution of strain along the range of stress up to the assumed failure strain of 17%.

Now those values are transferred to engineering values (Figure 14 and Table 3). The methodology of the transfer is explained in Appendix 3.

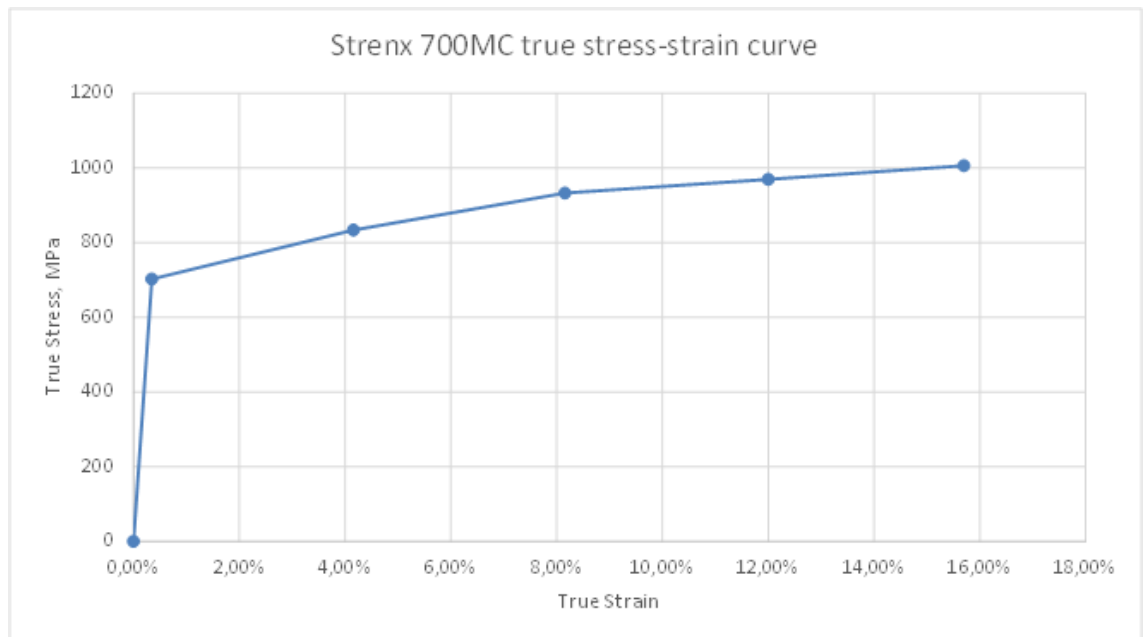


Figure 14. True stress-strain of Strenx 700MC

Table 3. Input parameters for the curve in Figure 14

True Strain	True Stress
0,00%	0
0,35%	702,45
4,16%	834
8,16%	933,1
12,00%	969,65
15,70%	1006,2

From true stress and strain, effective plastic stress and strain are calculated, by subtracting elastic deformation from plastic deformation.

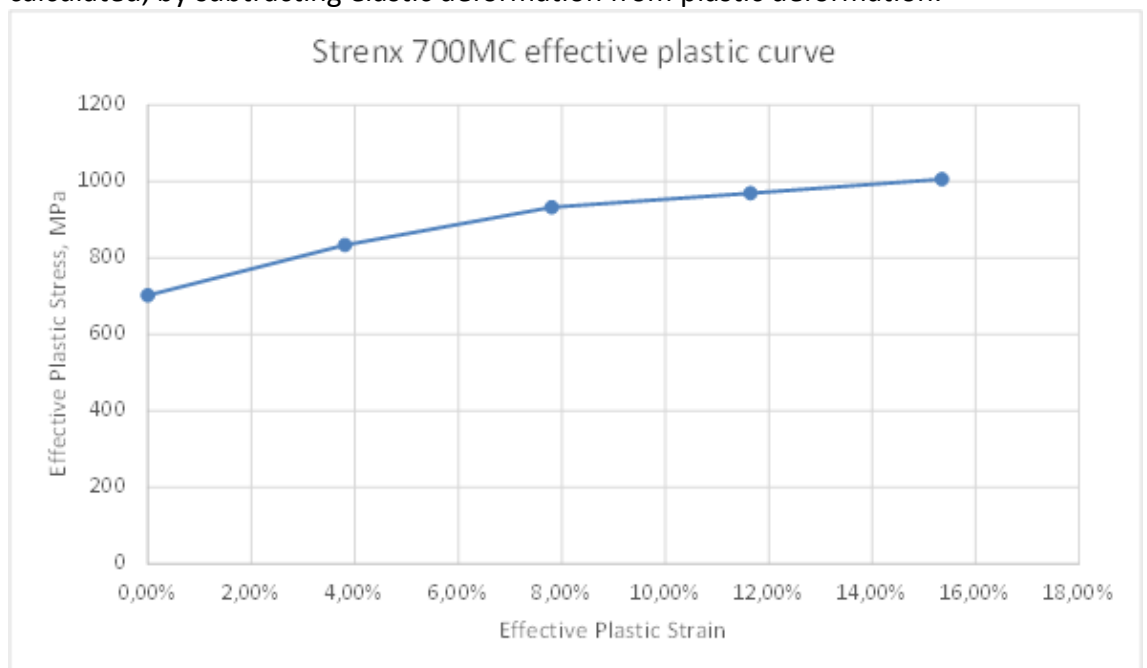


Figure 15. Effective plastic properties of Strenx 700MC

Table 4. Input parameters for the curve in Figure 15

Eff. Plastic strain	Eff. Stress
0,00%	702,45
3,81%	834
7,81%	933,1
11,65%	969,65
15,35%	1006,2

After producing the effective plastic values (see Figure 15 and Table 4), they can be input into the model in LS-PrePost in the following form for "MAT024 Piecewise Linear Plasticity" with the following units - *kg, mm, ms, kN, GPa, kN*mm* – shown in Figure 16:

The screenshot shows the 'Keyword Input Form' for 'MAT024 Piecewise Linear Plasticity'. The title is 'Strenx 700'. The form contains the following input fields:

MID	RO	E	PR	SIGY	ETAN	FAIL	TDEL
1	7.800e-06	200.00000	0.3000000	0.7024500	0.0	0.1535000	0.0

Additional parameters include:

- C: 0.0, P: 0.0, LCSS: 0, LCSR: 0, VP: 0.0
- EPS1: 0.0, EPS2: 0.0381000, EPS3: 0.0781000, EPS4: 0.1165000, EPS5: 0.1535000, EPS6: 0.0, EPS7: 0.0, EPS8: 0.0
- ES1: 0.7024500, ES2: 0.8340000, ES3: 0.9331000, ES4: 0.9696500, ES5: 1.0060000, ES6: 0.0, ES7: 0.0, ES8: 0.0

Buttons at the bottom include Plot, Raise, New, and Padd. Summary statistics at the bottom indicate: Total Card: 3, Smallest ID: 1, Largest ID: 3, Total deleted card: 0.

Figure 16. Strenx 700MC input parameters

A detailed explanation of input parameters is given in Appendix 5.

2.3.2 Filler material transformation

Filler material is a critical part of a welded joint. It has to be chosen with care and have an appropriate strength, either matching or higher than connected parts. In this case, we have a name of a filler material, available from previous theses - "OK ARISTOROD 69". Figure 17 shows the tensile properties:

Typical Tensile Properties				
AWS 80Ar/20CO₂ (M21) As welded				
Elongation	Tensile Strength	Yield Strength	Stress Relieved Temperature	Stress Relieved Testing Time
17 %	805 MPa	715 MPa	-	-
EN 80Ar/20CO₂ (M21) As welded				
Elongation	Tensile Strength	Yield Strength	Stress Relieved Temperature	Stress Relieved Testing Time
19 %	800 MPa	730 MPa	-	-
EN 80Ar/20CO₂ (M21) Stress relieved				
Elongation	Tensile Strength	Yield Strength	Stress Relieved Temperature	Stress Relieved Testing Time
20 %	750 MPa	690 MPa	620 °C	15 hr

Figure 17. Engineering properties of the weld (ESAB)

For the needs of this thesis, the properties of the first presented filler material will be used, even though there is no direct implication of it in previous theses of this series.

Note that ultimate tensile strength of "OK ARISTOROD 69" is mostly lower than that of Strenx 700MC ($f_u=750\text{...}950$). In *Nguyen (2018)* an important part of analysis of welds done for S700, is dealing with an issue of the under matched filler material chosen for the test, making the weld a critical part of the joint.

Figure 18 shows is a nominal stress-strain curve for the filler material and Table 5 shows the input parameters:

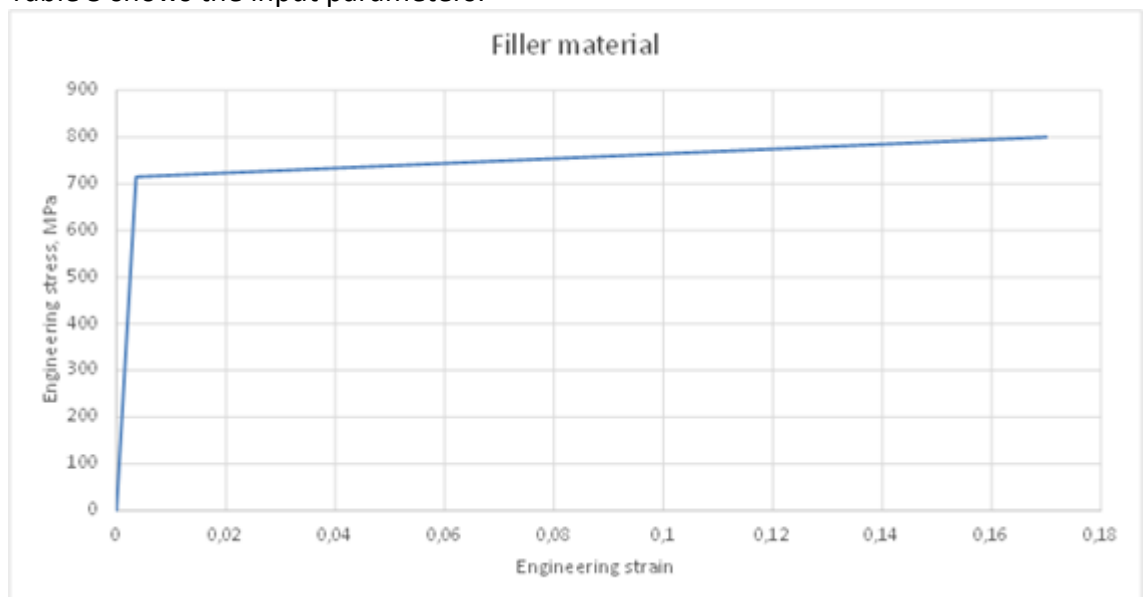


Figure 18. Engineering stress and strain of the filler material

Table 5. Input parameters for the curve in Figure 18

eng. strain	eng. stress
0	0
0,36%	715
17,00%	800

From engineering stress and strain, true stress and strain are calculated according to methodology given in Appendix 3.

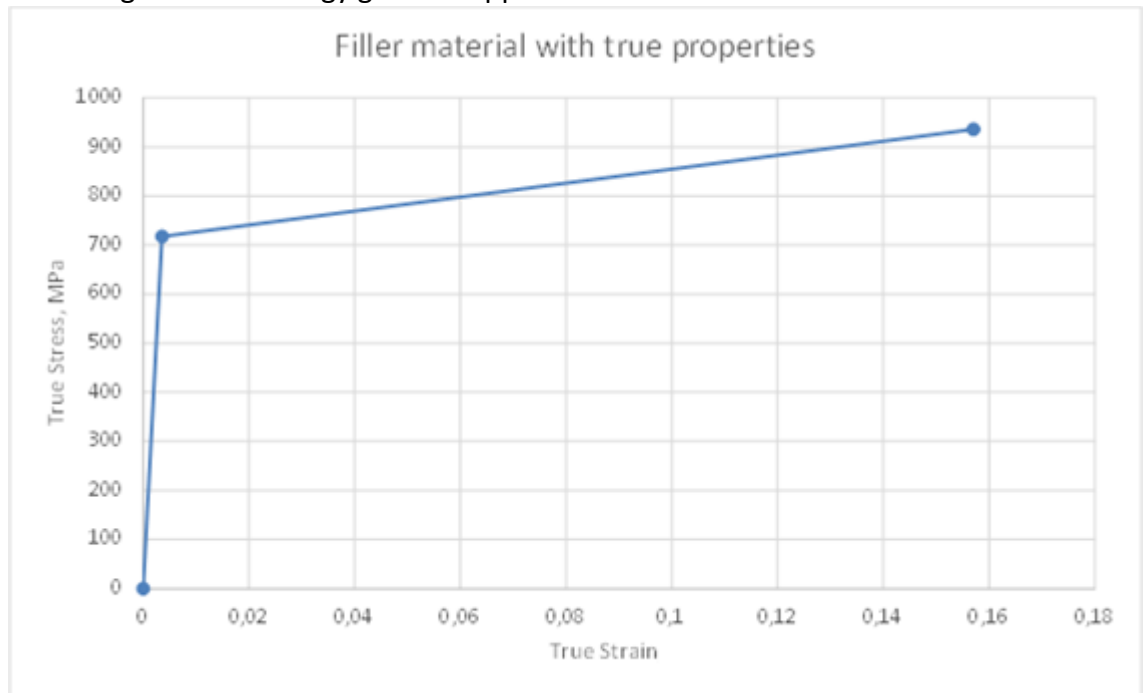


Figure 19. True stress and strain of the filler material

Table 6. Input parameters for the curve in Figure 19

True strain	True stress
0	0
0,36%	717,56
15,70%	936

From true stress and strain, defined in Figure 19 and Table 6, effective plastic stress and strain are calculated, by subtracting elastic deformation from plastic deformation as shown in Figure 20 and Table 7.

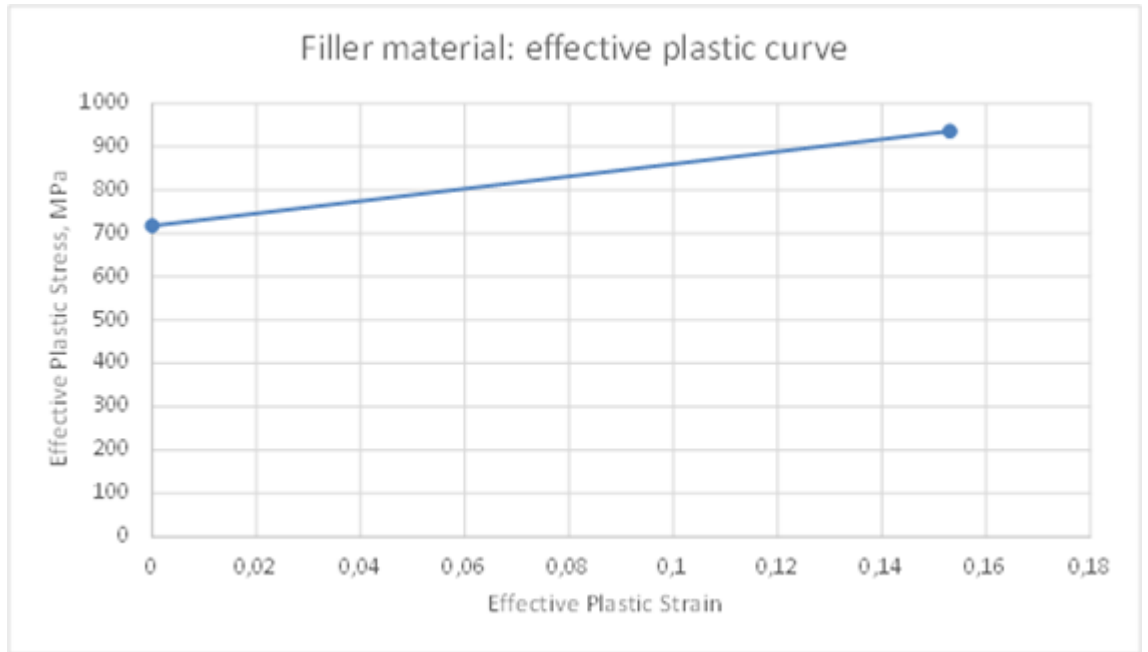


Figure 20. Effective plastic stress and strain of the filler material

Table 7. Input parameters for the curve in Figure 20

Eff. Plastic strain	Effective stress
0	717,56
15,30%	936

After producing the effective plastic values, input into the model in LS-PrePost can be done in the following form for "MAT024 Piecewise Linear Plasticity" with the following units - *kg, mm, ms, kN, GPa, kN*mm*:

Keyword Input Form

Use *Parameter
 Comment
 (Subsys: 1 F6F_2D_311018_ELF0RM12.k)

*MAT_PIECEWISE_LINEAR_PLASTICITY_(TITLE) (024) (3)

TITLE
Weld

1	<u>MID</u>	<u>RO</u>	<u>E</u>	<u>PR</u>	<u>SIGY</u>	<u>ETAN</u>	<u>FAIL</u>	<u>TDEL</u>
	2	7.800e-06	200.00000	0.3000000	0.7170000	0.0	0.1530000	0.0
2	<u>C</u>	<u>P</u>	<u>LCSS</u>	<u>LCSR</u>	<u>VP</u>			
	0.0	0.0	0	0	0.0			
3	<u>EPS1</u>	<u>EPS2</u>	<u>EPS3</u>	<u>EPS4</u>	<u>EPS5</u>	<u>EPS6</u>	<u>EPS7</u>	<u>EPS8</u>
	0.0	0.1530000	0.0	0.0	0.0	0.0	0.0	0.0
4	<u>ES1</u>	<u>ES2</u>	<u>ES3</u>	<u>ES4</u>	<u>ES5</u>	<u>ES6</u>	<u>ES7</u>	<u>ES8</u>
	0.7170000	0.9360000	0.0	0.0	0.0	0.0	0.0	0.0

Total Card: 3 Smallest ID: 1 Largest ID: 3 Total deleted card: 0

Figure 21. Filler material input parameters

Figure 21 shows used input parameters for the filler material.

A detailed explanation of input parameters is given in Appendix 5.

2.3.3 Heat-affected zone transformation

Heat affected properties are the hardest to determine. The process of determination requires a few general assumptions:

- Homogeneity of properties in all directions
- Uniformity of stress and strain throughout the thickness of HAZ

With those assumptions, stress and strain values can be pinned down.

The first problem is the stress value uncertainty. It is born from the process of formation of HAZ. *It is known (Martin, 1996)* that ultimate tensile stress of HAZ is lower than the strength of the parent material in case of HSS, because heat treatment applied through the process of welding stabilizes the parent material, making it weaker and coarser. Coarseness alone would be a problem in case of a normal structural steel, since it has stable metallurgy, keeping strength of the steel independent from heat treatment and thus welding procedure is focused on achieving good heat input, so the cooling process would allow the steel microstructure to stay similar to the parent material and to allow the fusion process to be finished. In case of HSS, welding procedure has also to focus on putting a maximum limit on a singular heat input, so steel microstructure does not degenerate from unstable HSS microstructure down to a stable one of a structural steel, thus weakening it, at the same time keeping the grain size of a microstructure in adequate limits. This is why it is hard to achieve appropriate welding parameters for HSS.

More information about this huge problem can be found in theses by *Grecevci (2016)* and *Nguyen (2018)* as well as in *SSAB Strenx Welding Guide*.

The Second problem in the definition of f_u of HAZ is its unevenness. In Figure 22, you can see an idealized formation of HAZ, forming equally on both sides of the weld.

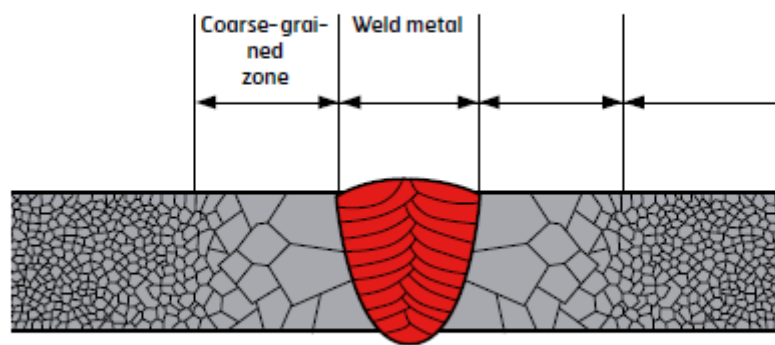


FIGURE 8 Coarse-grained zone of HAZ.

Figure 22. Example of HAZ formation (SSAB Strenx Welding Guide)

Naturally, it is not entirely so, even though heat propagates through steel equally in all directions, the direction of the heat input and local reaction of tempered steel is not always evenly distributed. The same goes for the cooling process. As shown by previous theses in this series (*Grecevcı (2016)*; *Abebe (2016)*; *Nguyen (2018)* and *Giraldo (2018)*), no two specimens made by the same welder and water cut from the same welded specimen yield similar failure results.

It is easier to see the lack of uniformity in the results of *Nguyen* rather than in *Giraldo*, because test arrangement of *Nguyen (2018)* is straightforward, unlike the complexity of *Giraldo (2018)*.

Although, all of the empirical evidence from previous theses points to the lack of uniformity in HAZ failure stress (due to significant differences in strain as well as with above mentioned reasons), it is assumed that it is uniform both in longitudinal and perpendicular directions, akin to a well manufactured steel. It is possible to make this assumption, because there is no other option, since unevenness of failure stress in HAZ cannot be measured, but only the predicted based on the tensile tests, faith in good welding procedures and favorable results.

There are nine options for the definition of nominal properties of HAZ conceived for this thesis. One stress option and one strain options are derived from tests by *Giraldo (2018)* and supported by the results of *Nguyen (2018)*. Other two options for strain and two options for failure stress are chosen based on meetings with Ma and Havula (*Meeting on 08.11.2018*).

Since failure strain of Strenx 700MC was destined at 17%, in order to accommodate the failure strain of the filler material. Failure strain of HAZ is chosen to be the same as in parent material. This decision is based on a

prolonged discussion with Ma (*Meeting on 20.11.2018*), regarding strain values of steel and changes in properties of HAZ. Therefore, an educated guess of uniformity of strain values between HAZ and parent material is made.

In the same interview with Ma (*Meeting on 20.11.2018*), two models for an exploratory definition of good stress properties for HAZ were suggested: by using a full strength of parent material, to get the top limit of HAZ properties (and thus of a whole model), and by using a 90% of f_u of the parent material, to get an approximate value of HAZ yield and ultimate strength (based on a common assumptions regarding HAZ f_u).

Following Figure 23 and Table 8 show the nominal properties of 90% HAZ stress-strain curve and parameters used in its definition.

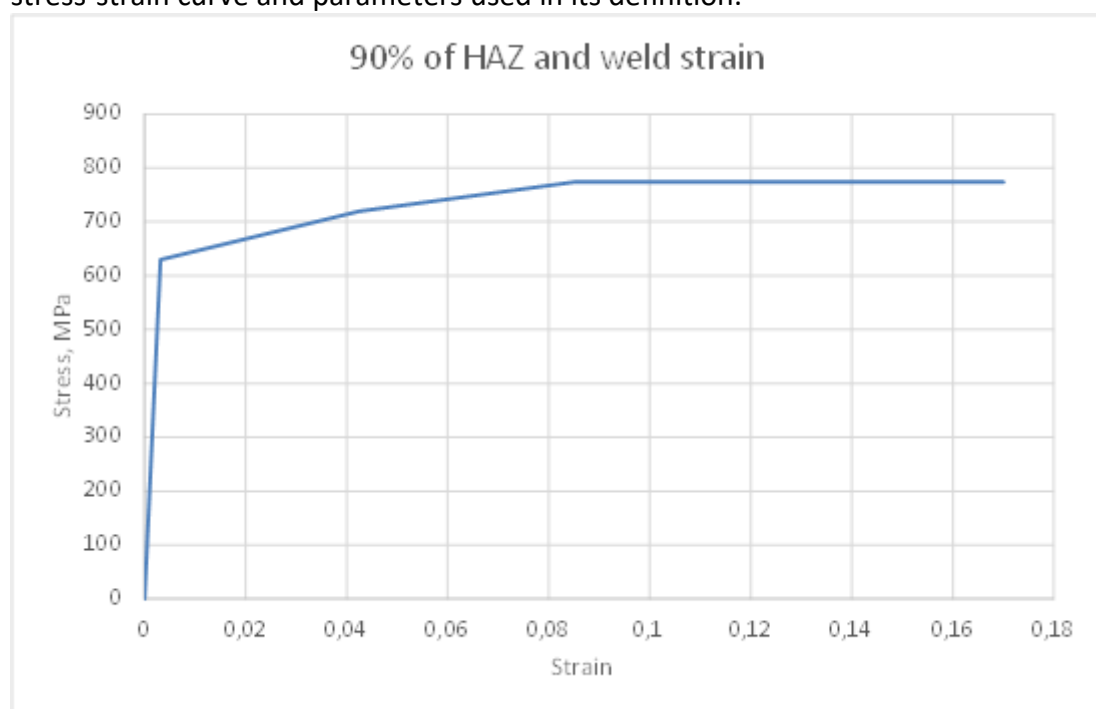


Figure 23. HAZ stress-strain curve with 90% f_u of parent material

Table 8. Input parameters for the curve in Figure 23

eng. strain	eng. stress
0	0
0,32%	630
4,25%	720
8,50%	774,00
12,75%	774
17,00%	774

However, even though we have a suggestion for HAZ failure stress, results of *Giraldo (2018)* for the specimen F6_1 and results of *Nguyen (2018)* for S700 (S700-1R-2 specifically), show a good failure stress correlation with each other. The value of failure strain for HAZ in both cases is about 630

N/mm² (Figure 24 and Table 9 demonstrate the correlation). This gives a good reason to consider this value, but causes a necessity for a series of exploratory simulations, in order to check for correlations with F6_1 failure mode and the load-displacement graph of the F6_1 specimen.

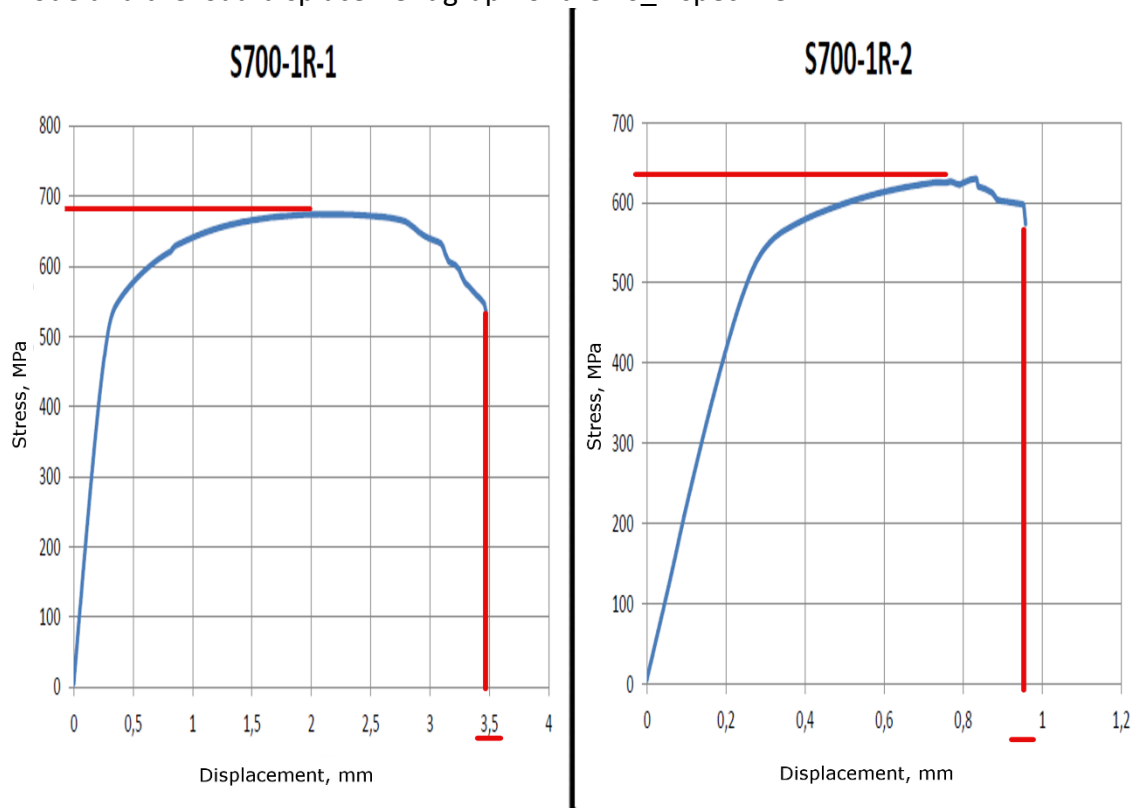


Figure 24. Compiled S700 results from *Nguyen (2018)*

In addition to tensile tests, *Nguyen (2018)* supports his results with Vickers hardness tests and a rough conversion between hardness values and ultimate tensile stress, yielding a result of about 695 MPa with hardness value of 212. Yet, there is a problem with this measurement - it is based on conversion tables for carbon steel, not HSS. Therefore, there is no direct correlation, only an indirect one.

As for the test values of *Giraldo (2018)*, adjustments have to be made. The idea of it is to transfer value of stress recorded in the test into a smaller area of the weld, since fillet weld with a leg of 6 mm is smaller than HSS plate with thickness of 8 mm. The process is shown in Table 9.

Table 9. Translation of stress values for F6_1

A=8mm * 1mm	A=6mm * 1mm		
MPa	MPa		
Failure stress:	Failure stress:		Increase:
467,26	623,01		33%

Therefore, the test based strain curve with weld based strain looks like the one on Figure 25 and Table 10:

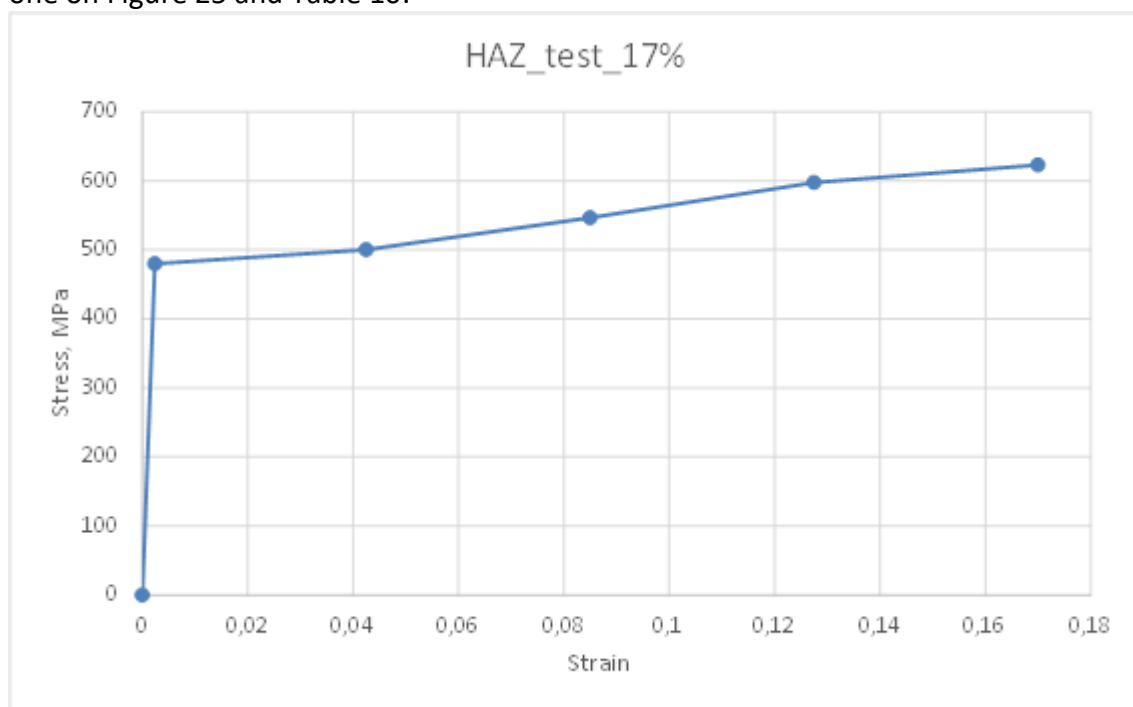


Figure 25. HAZ stress-strain curve with stress values from *Giraldo (2018)*

Table 10. Input data for the curve in Figure 25

eng. strain	eng. stress
0	0
0,24%	480
4,25%	500
8,50%	546,67
12,75%	597,33
17,00%	623

In order to justify the choice between two concepts of ultimate tensile stress for the final model, a previously mentioned model runs were analyzed. Figure 26 shows a comparison of failure sequences and load-displacement graphs of those models.

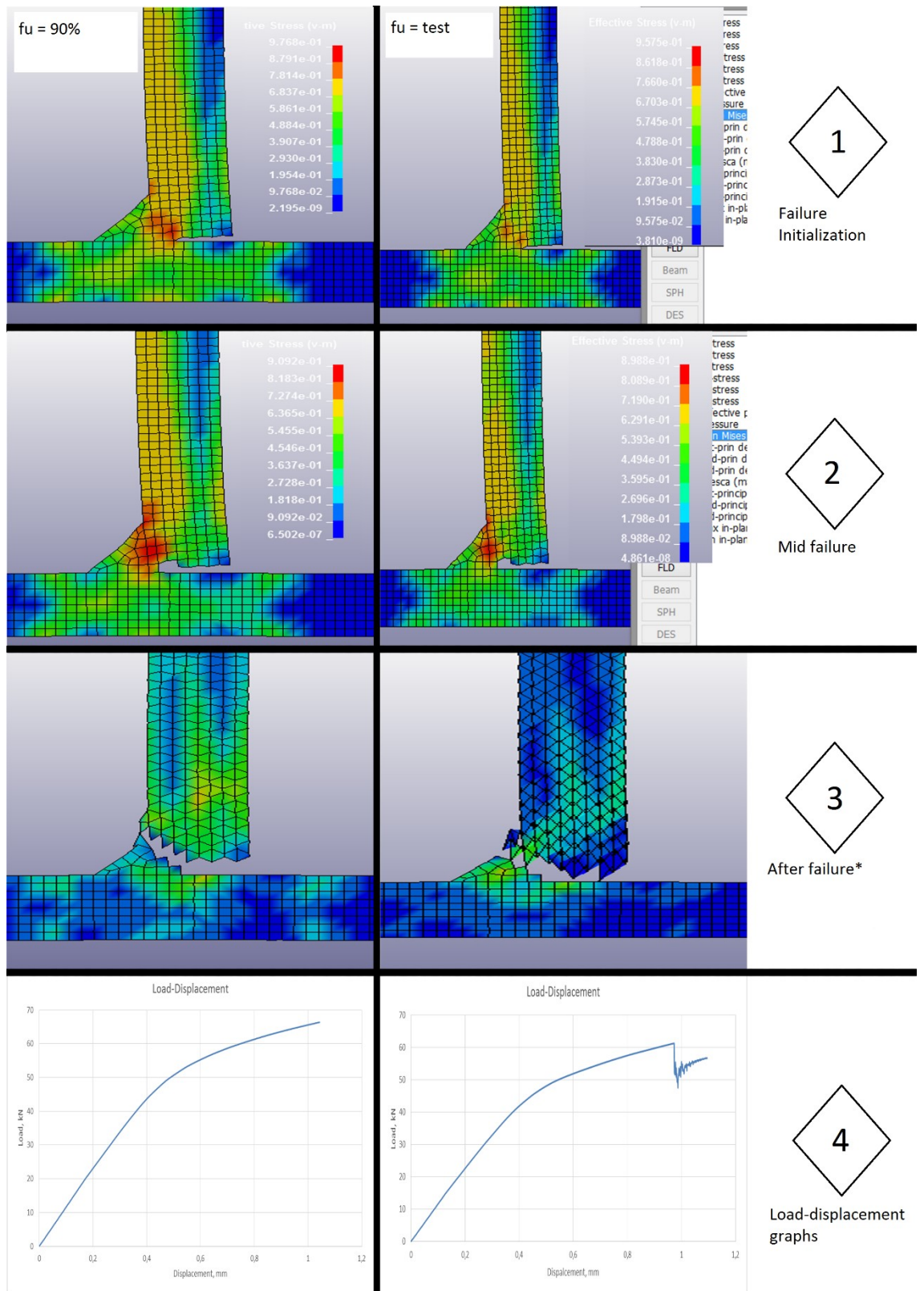


Figure 26. Comparison of failure modes and displacement graphs

*After failure, strange state of shells is covered in the section on modelling. It does not have an effect on the maximum load in load-displacement graphs. The effect can be fixed by the addition of *Hourglass keyword with

standard settings into the model. See *LS-Dyna User's Manual Volume 1* for more information.

As can be seen in Figure 26, the maximum load of 90% stress model is about 66 kN and maximum load of the test based stress model is about 61 kN. Displacement is similar - 1 millimeter. Failure modes are almost identical (NB! Oversized elements were used for test runs due to economic reasons).

Based on the results of the model runs, analysis of studies of *Giraldo (2018)* and *Nguyen (2018)* and discussions with thesis supervisors (see list of interviews), test based stress model was chosen as shown in Figure 27.

With the test based stress-strain curve for HAZ, true stress and strain values can be calculated, according to Appendix 3 (Figure 27 and Table 11).

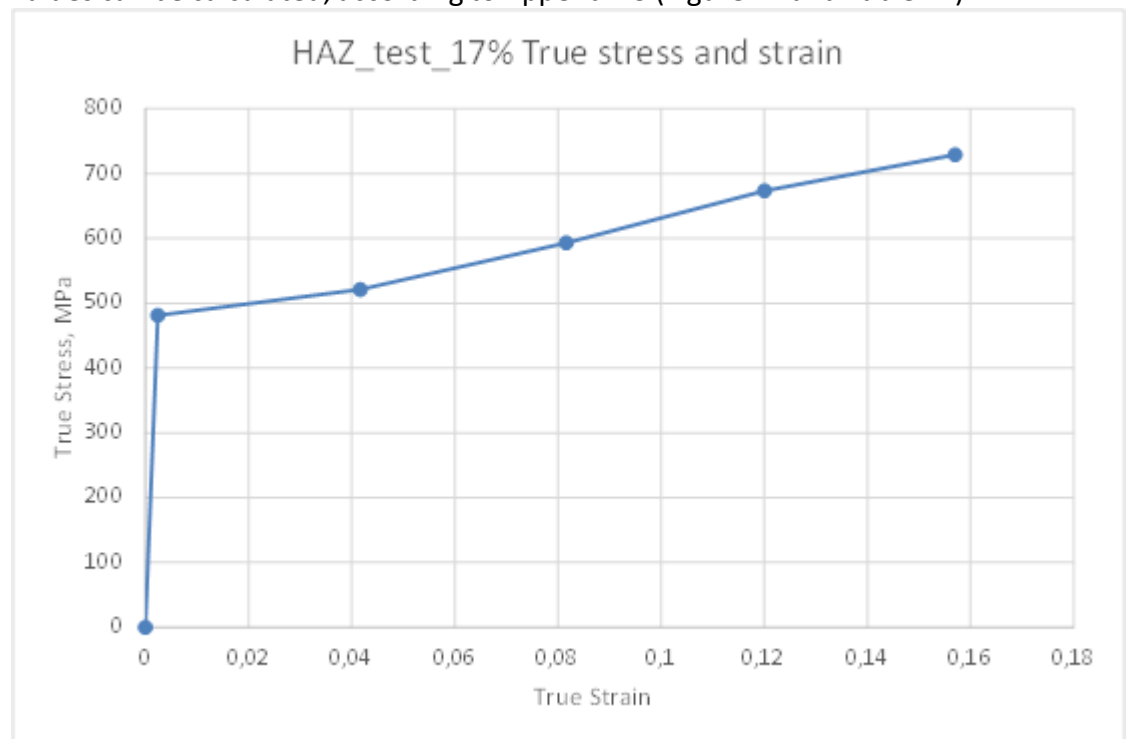


Figure 27. True stress-strain curve for HAZ

Table 11. Input parameters for the curve in Figure 27

True strain	True stress
0	0
0,24%	481,152
4,16%	521,25
8,16%	593,13333
12,00%	673,48958
15,70%	728,91

From true stress and strain, effective plastic stress and strain are calculated, by subtracting elastic deformation from plastic deformation (see Figure 28 and Table 12).

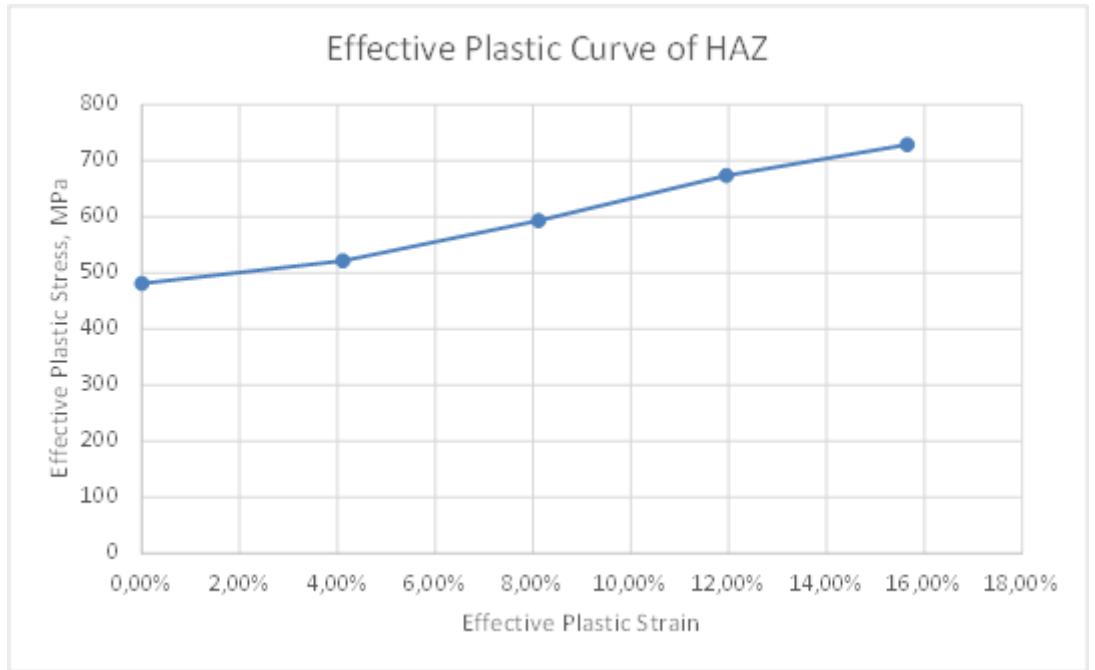


Figure 28. Effective plastic properties of HAZ

Table 12. Input parameters for the curve in Figure 28

Eff. Plastic strain	Eff. Stress
0,00%	481,152
4,11%	521,25
8,11%	593,1333
11,95%	673,4896
15,65%	728,91

After producing the effective plastic values, they can be inputted into the model in LS-PrePost in the following form for "MAT024 Piecewise Linear Plasticity" with following units - kg, mm, ms, kN, GPa, kN*mm:

Keyword Input Form

MatDB RefBy Pick Add Accept Delete Default Done

Use *Parameter Comment (Subsys: 1 F6F_2D_311018_ELF0RM12.k) Setting

*MAT_PIECEWISE_LINEAR_PLASTICITY_(TITLE) (024) (3)

TITLE
HAZ

1	MID	RO	E	PR	SIGY	ETAN	FAIL	TDEL
	3	7.800e-06	200.00000	0.3000000	0.4810000	0.0	0.1565000	0.0
2	C	P	LCSS	LCSR	VP			
	0.0	0.0	0	0	0.0			
3	EPS1	EPS2	EPS3	EPS4	EPS5	EPS6	EPS7	EPS8
	0.0	0.0411000	0.0811000	0.1195000	0.1565000	0.0	0.0	0.0
4	ES1	ES2	ES3	ES4	ES5	ES6	ES7	ES8
	0.4810000	0.5210000	0.5930000	0.6730000	0.7280000	0.0	0.0	0.0

Plot Raise New Padd

Total Card: 3 Smallest ID: 1 Largest ID: 3 Total deleted card: 0

Figure 29. HAZ input parameters

Used input parameters are given in Figure 29.

A detailed explanation of input parameters is given in Appendix 5.

2.4 Load, support conditions and load path

This chapter covers a description of load definition and application as well as definition of support conditions.

2.4.1 Load application in LS-Dyna

In LS-Dyna load can be applied by three methods: through displacement, velocity or acceleration. The main keyword for that is `*Boundary Prescribed Motion Set`, which allows to move a predefined set of nodes in any major direction.

In case of tests described in *Giraldo (2018)*, the load is applied through the top part of the specimen, by two claws gripping it from both sides. See Figures 30 and 31.

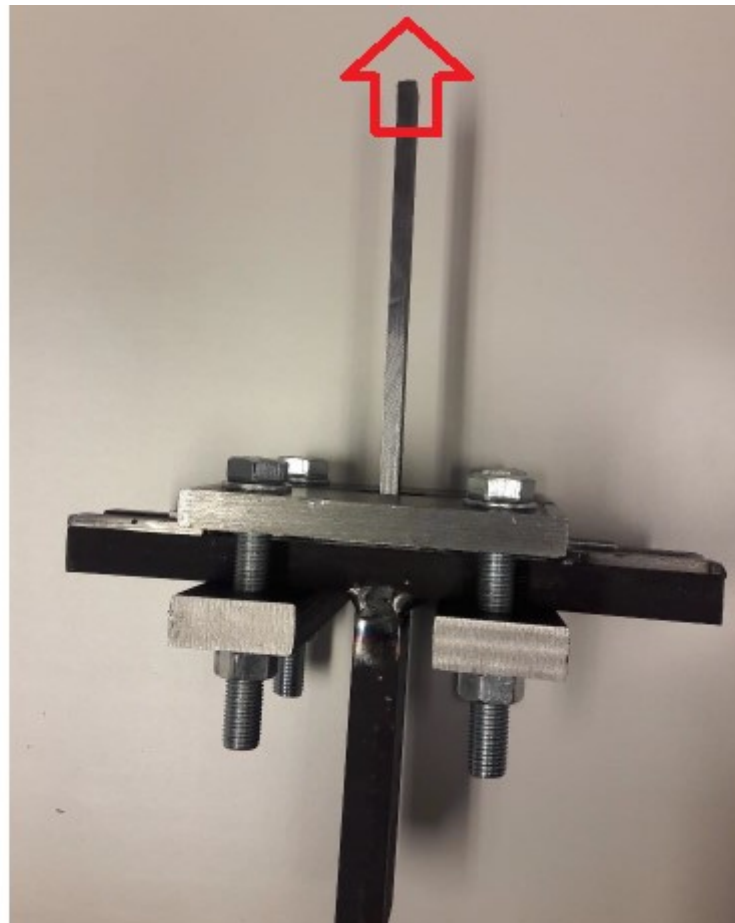


Figure 30. Test arrangement of Giraldo (2018)



Figure 31. Arrangement of *Giraldo (2018)* in testing

In case of modelling, a simplification can be introduced - load application through the cross section of the top plate. In this way the displaced nodes are moved uniformly in one direction (Figure 32 illustrates this argument).

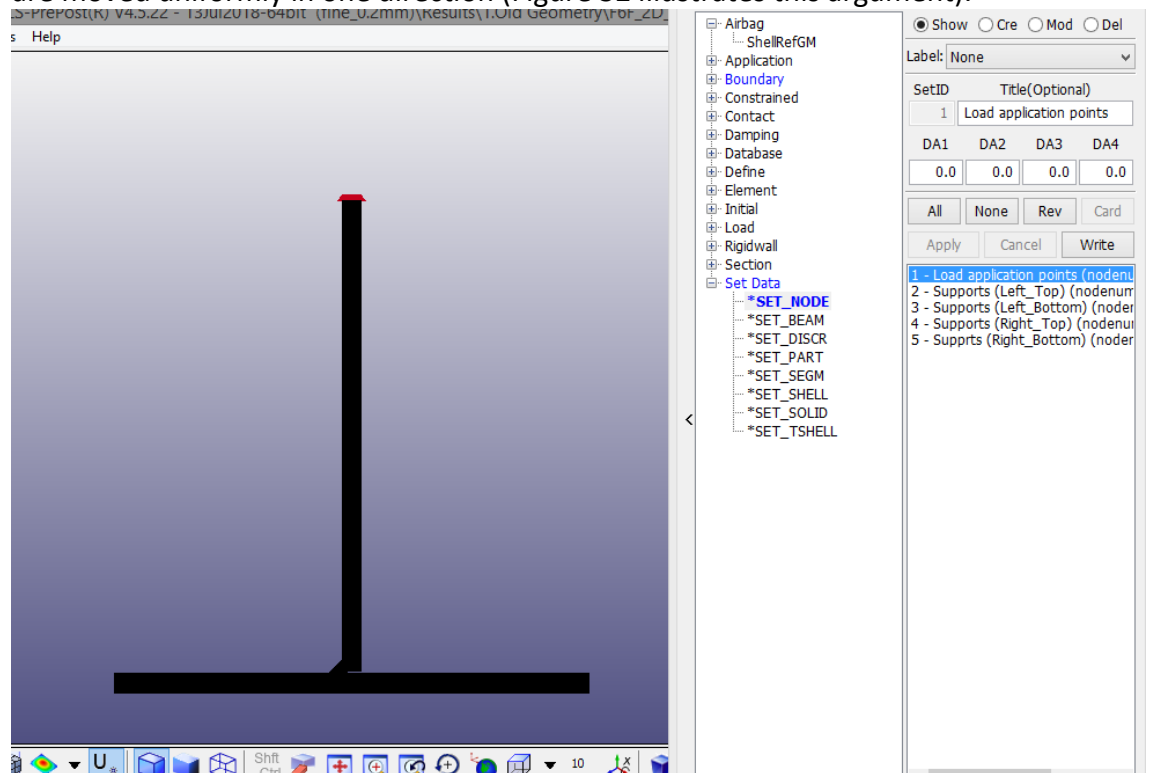


Figure 32. Load application points

In this thesis, load application is done through the displacement (Figure 33).

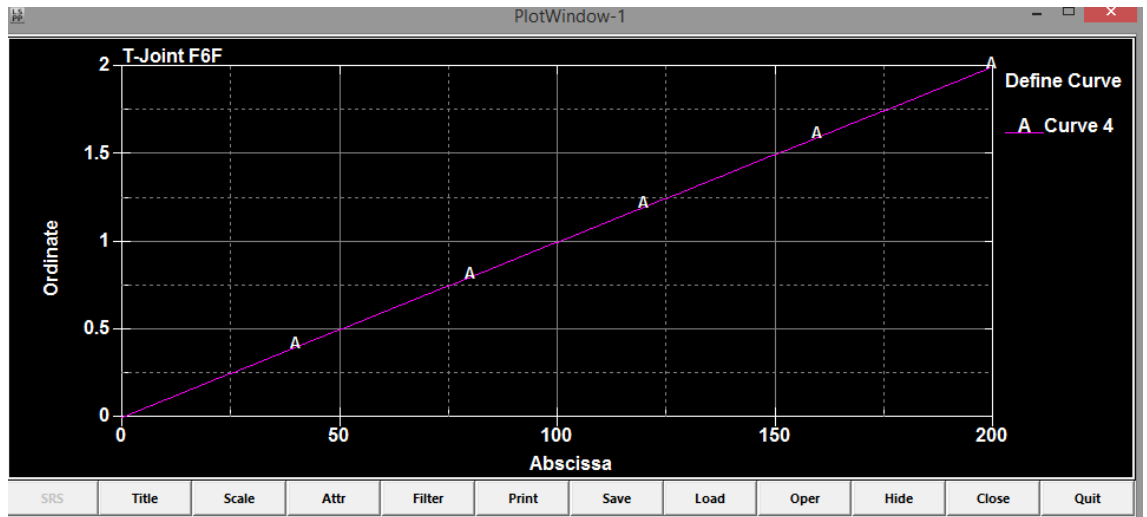


Figure 33. Displacement/time graph

Ordinate shows millimeters and abscissa shows milliseconds. Such a relatively slow time step (0.01 mm/ms) is defined so that the final result is not subject to dynamic effects, in order to keep the load application static and thus true to applications in construction engineering. The presence of dynamic effect can be checked on the output load-displacement graph by presence (or lack of) high frequency nonlinearities.

Note that displacement is measured in millimeters and time in milliseconds. It is done so, in order to conform to *GMAT* unit system (kN, mm, ms, kg, GPa). Since LS-Dyna does not have an automatic definition of units, it has to be kept in mind while preparing the data for input and while analyzing the output.

The maximum displacement of the top nodes used in this thesis is 2 millimeters. At this point, the failure is achieved, while in results of *Giraldo (2018)* measured displacement at failure is 6-7 millimeters. This curiosity is covered in Appendix 2. Example is shown in Figure 34.

The figure shows a 'Keyword Input Form' window. At the top, there are buttons: NewID, Draw, Pick, Add, Accept, Delete, Default, Done. Below these are checkboxes for 'Use *Parameter' and 'Comment', and a 'Setting' button. The main area contains a table with the following data:

ID	TITLE	NSID	DOF	VAD	LCID	SF	VID	DEATH	BIRTH
0	Load	1	2	2	4	1.0000000	0	1.000e+28	0.0

Below the table is a 'COMMENT:' field and a status bar at the bottom that reads: 'Total Card: 1 Smallest ID: 1 Largest ID: 1 Total deleted card: 0'.

Figure 34. Keyword parameters for the load

2.4.2 Support conditions

Real support conditions of *Giraldo (2018)* are shown in Figure 30.

From those support conditions, a simplification can be made for modelling shown in Figure 35. The support conditions are limiting vertical and lateral movements in assigned node sets on top and bottom of the base plate (bottom nodes are redundant, but do not change the load path).

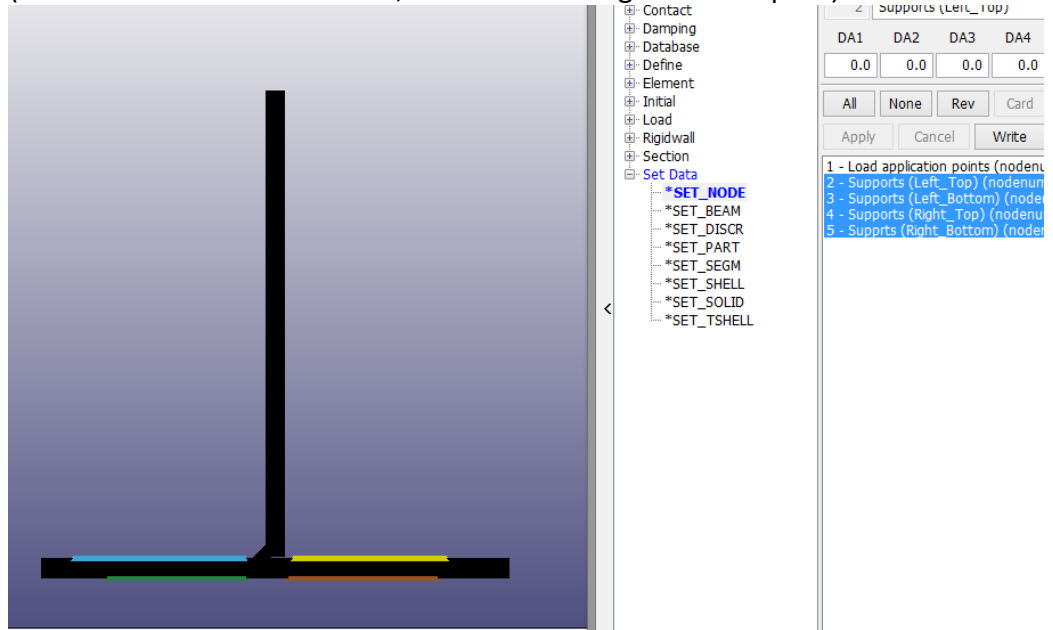


Figure 35. Support conditions in the model

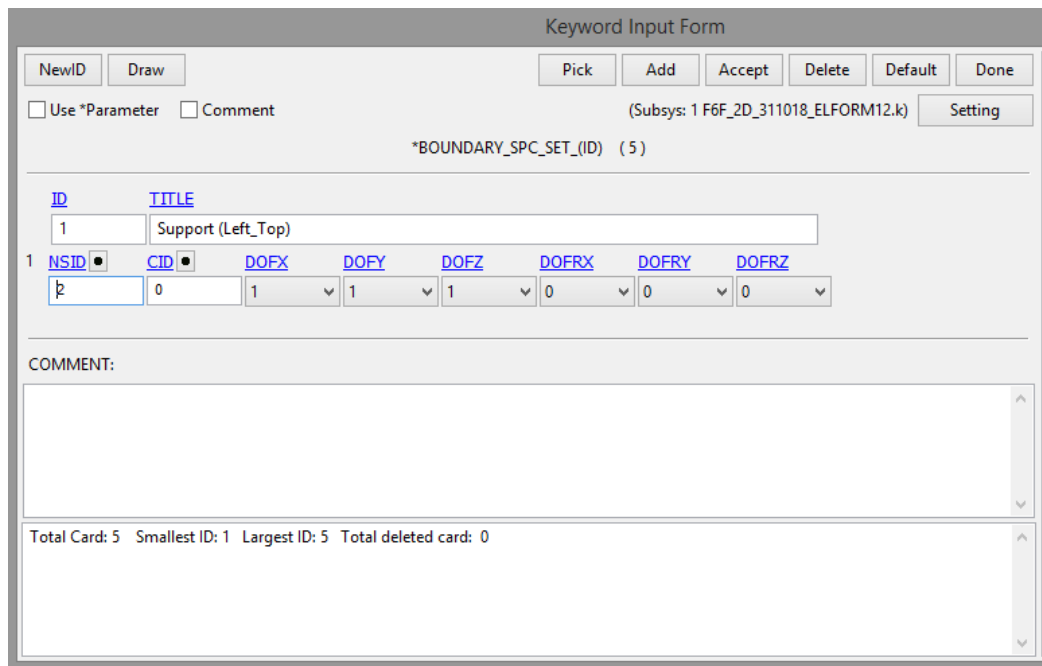


Figure 36. Keyword parameters for the supports

Used keyword parameters are shown in Figure 36.

Additional explanation of definition of the supports can be found in (*LS-Dyna User's Manual Volume 1*)

2.5 Final model geometry and hardware limitations

After dealing with preliminary calculations, an improved model geometry was constructed. It was a necessary improvement, due to hardware limitations on HAMK computers - the model was simply calculating for too long, for over 14 hours. So an improved set up was devised (shown in Figure 37).

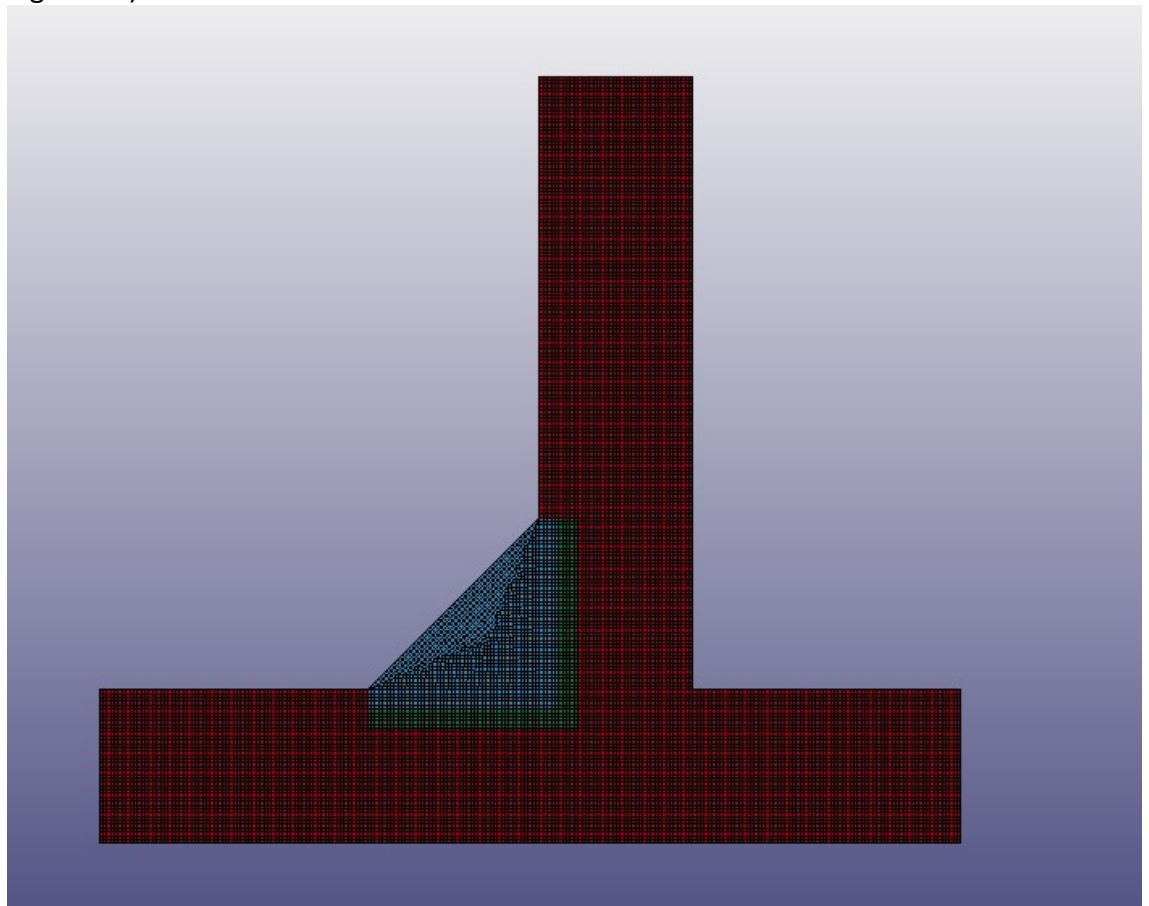


Figure 37. Improved model

The model is radically shorter than the original one, but it does not change the load path. Since planned supports of *Giraldo (2018)* start almost at the weld zone, the rest of the specimen becomes unnecessary for a proper simulation of the failure. Apart from shortening of the plates, the element size was reduced from 1 mm down to 0,2 mm, creating a better failure simulation. Support nodes were slightly tweaked as shown in Figure 38, while restriction parameters were left the same as in the original model. Load application parameters were left similar to the original model,

without any directional restraints apart from programmed nodal displacement upward.

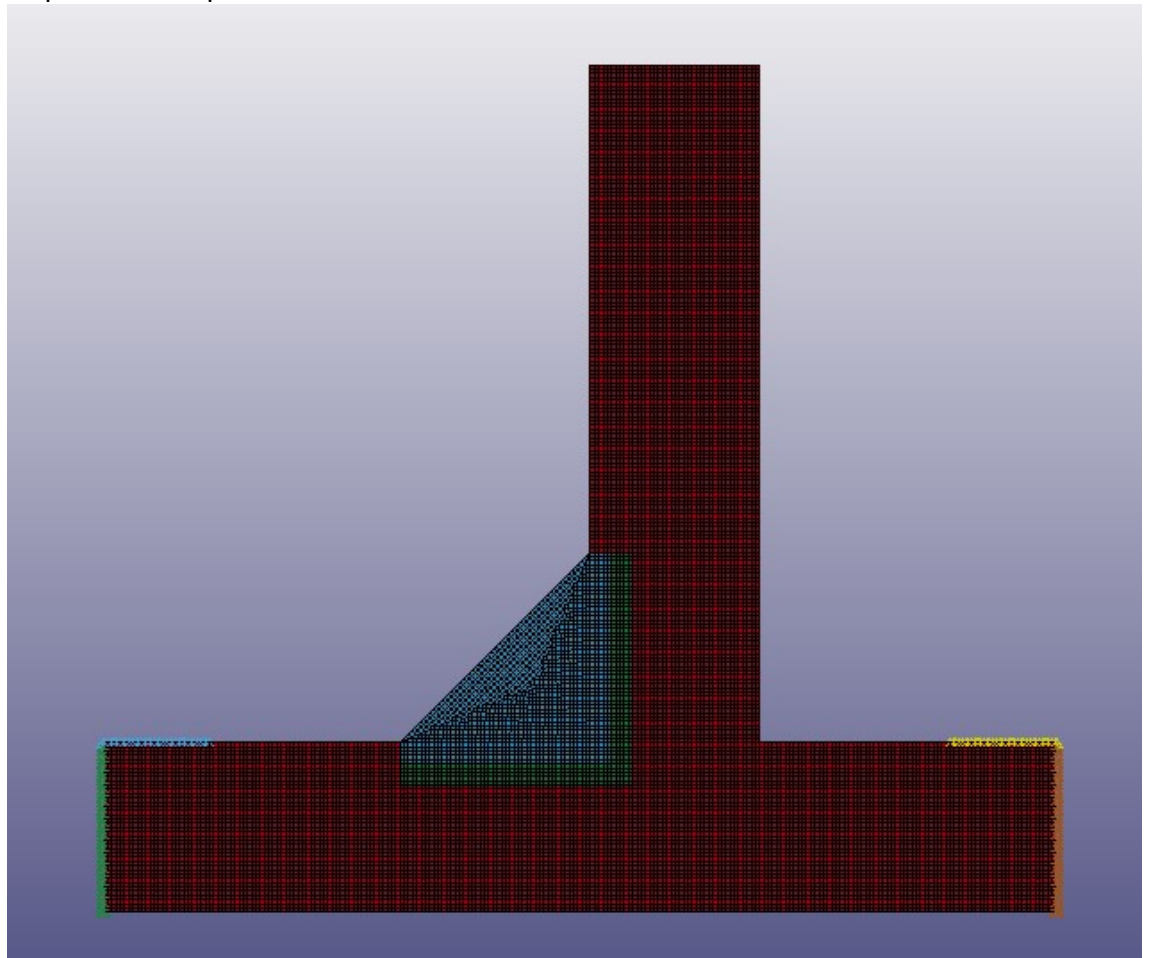


Figure 38. Support nodes of the improved model

3 ANALYSIS OF THE SIMULATION OF IMPROVED MODEL

This section covers an analysis of the modelling results based on double criteria:

- Similarity of failure mode between specimen and model
- Similarity of load displacement graphs of specimen and model

Therefore, two points of comparison - visual and measured/observed.

Figure 39 presents the failure mode of the specimen F6_1 from *Giraldo (2018)*.

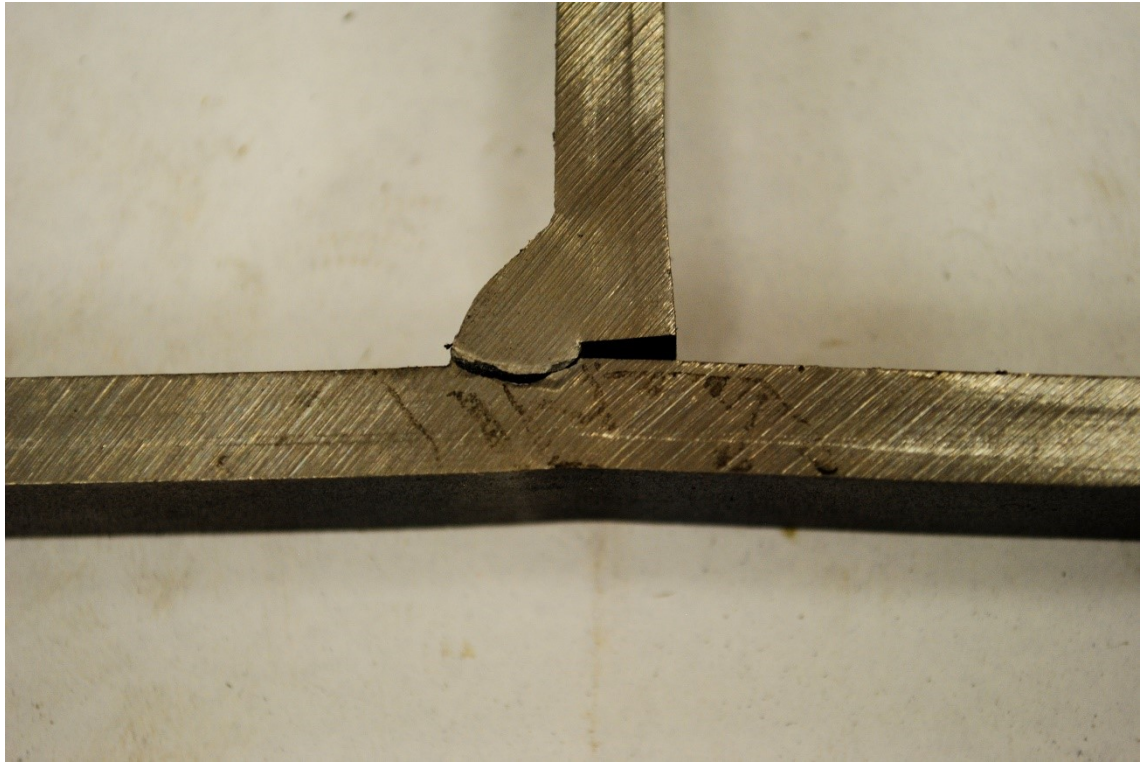


Figure 39. Specimen F6_1 Failure mode

The failure happened along the approximate borderline between HAZ and parent material in the bottom plate. With visible deformations in the bottom plate and along the upper leg of the weld and adjusted region of HAZ, indicating a developing plastic hinge.

The failure mode of the model is shown in the Figures 40 to 46.

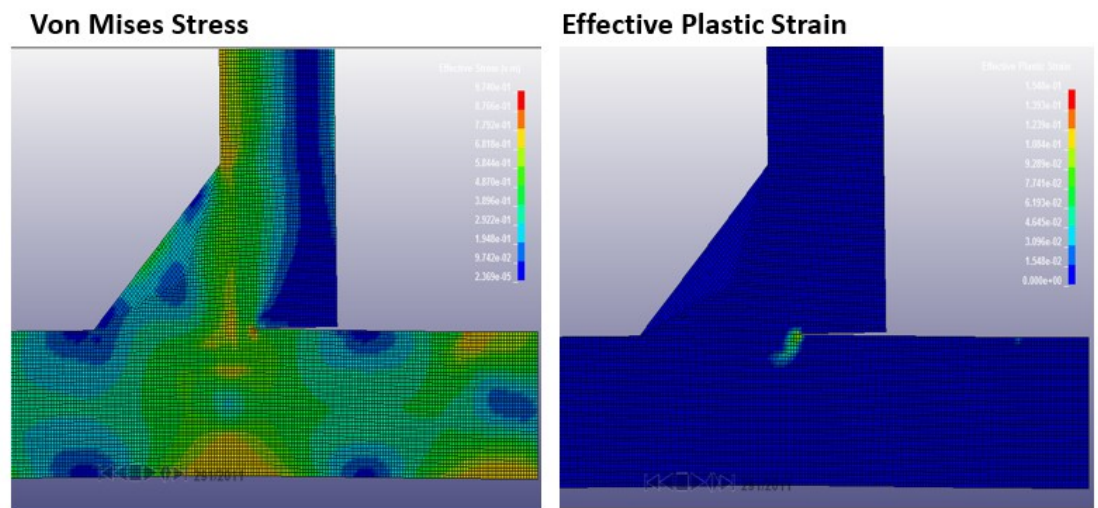


Figure 40. Failure initialization (vertical displacement +0.29 mm)

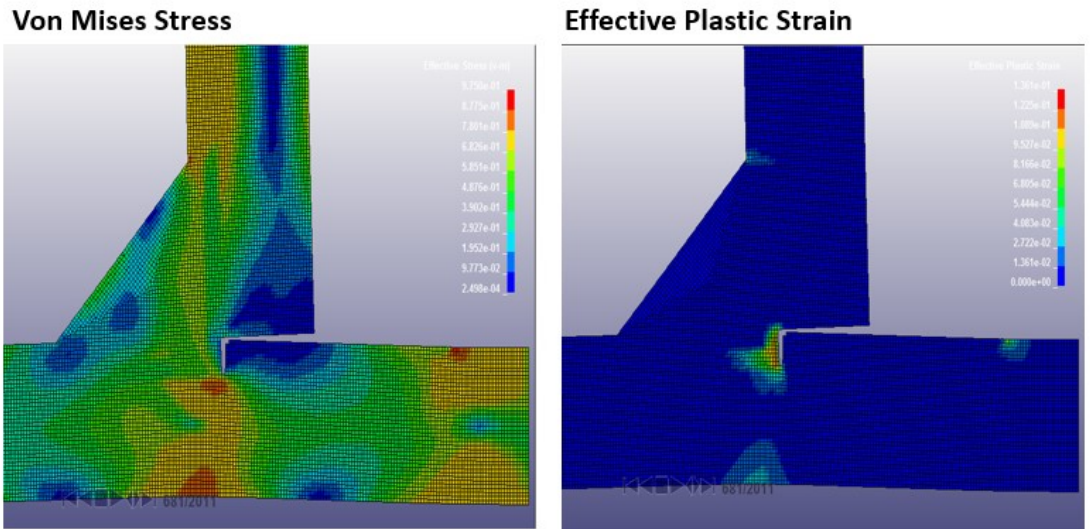


Figure 41. Failure Progression State 1 (vertical displacement +0.68 mm)

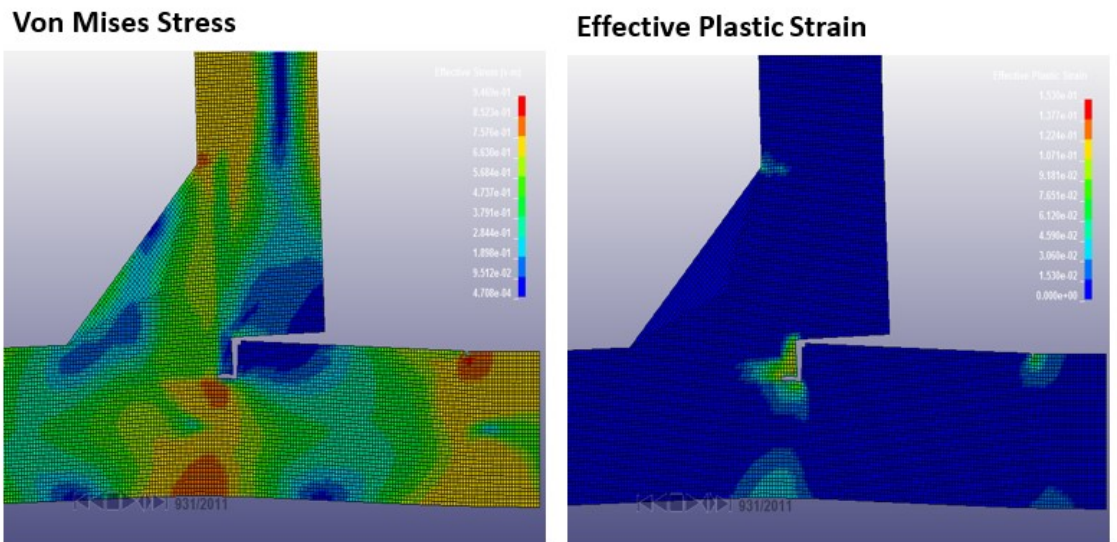


Figure 42. Failure Progression State 2 (vertical displacement +0.93 mm)

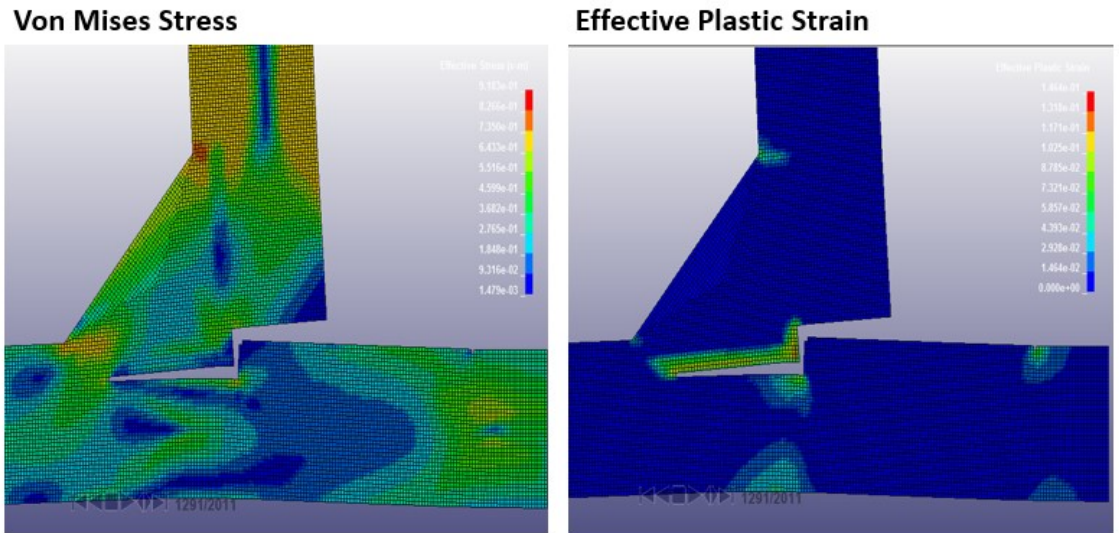


Figure 43. Failure Progression State 3 (vertical displacement +1.29 mm)

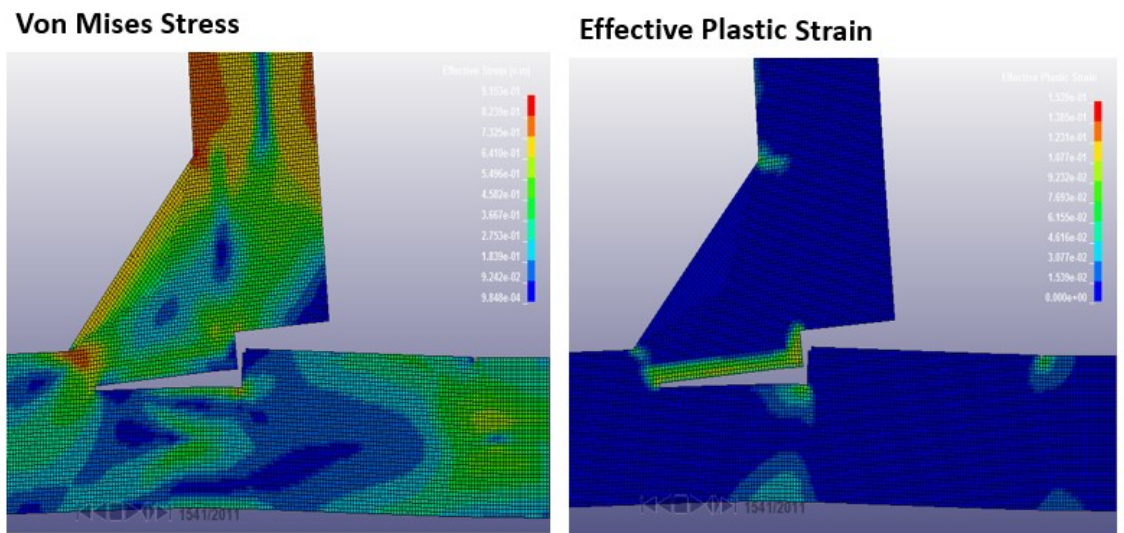


Figure 44. Failure Progression State 4 (vertical displacement +1.54 mm)

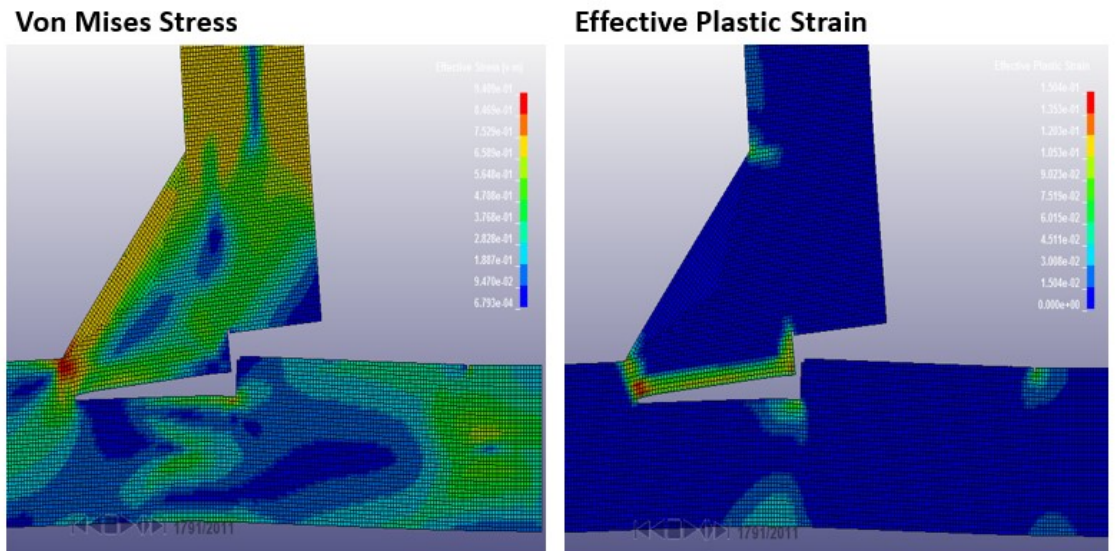


Figure 45.
mm)

Pre Failure State (vertical displacement +1.79

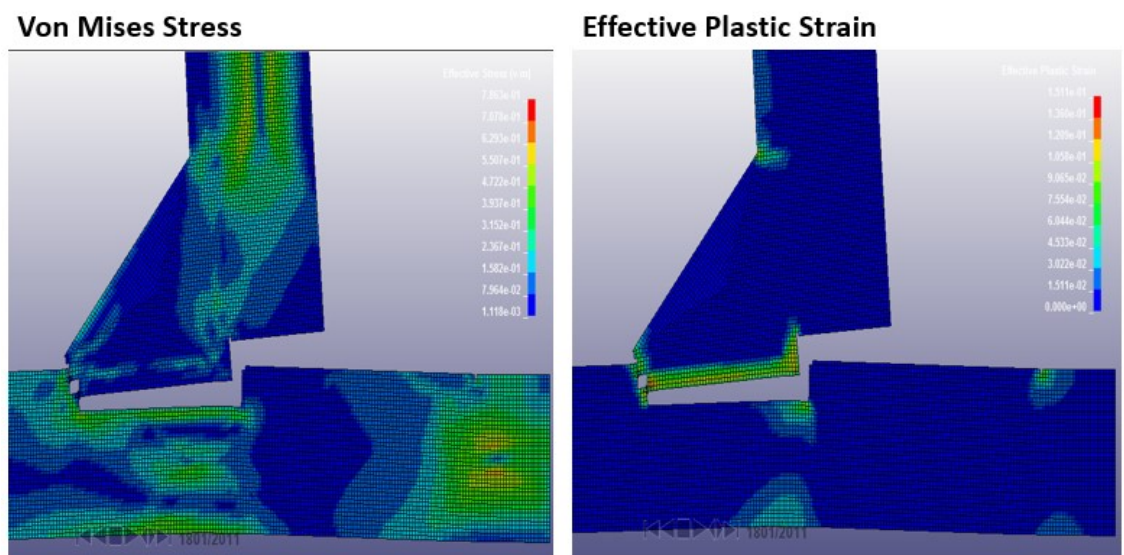


Figure 46.
mm)

Post Failure State (vertical displacement +1.8

As can be seen in Figures 40 to 46, the failure pattern produced by the simulation is quite close to F6_1 of *Giraldo (2018)*. The failure happens at the bottom plate, leaving a plastic deformation in the bottom plate and at the top of the weld leg. The fault line goes on the border between HAZ and parent material, conforming to the proposed idea of the fault line. The difference between the model and specimen in this regard is the shape of HAZ - in the specimen it should be a radial shape, depending on the real heat input and welding position. Figure 47 shows the load-displacement graph of the model.

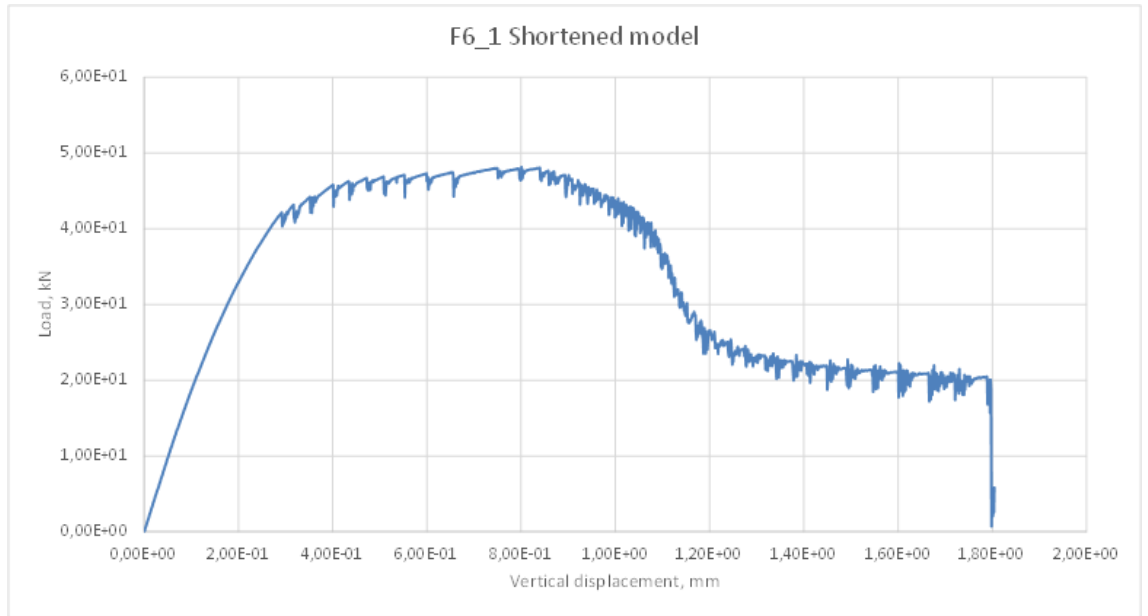


Figure 47. Load-displacement graph of the improved model

The maximum load exerted on the model by imposed displacement reaches a value of about 48 kN. At that, the model shows signs of dynamic impact with a start of the plastic deformation and subsequent failure. However, it is a natural result of the ripping failure pattern. With reduced contact area, the stress concentration on the fault line increases and reduces the required load for each subsequent deletion of a shell element.

If a faster, less balanced displacement application or a reduction of the required effective plastic strain parameter for the materials was used, then the failure would have been more abrupt. Like in the specimen that this model is based on. See Figure 48 for its load-displacement graph.

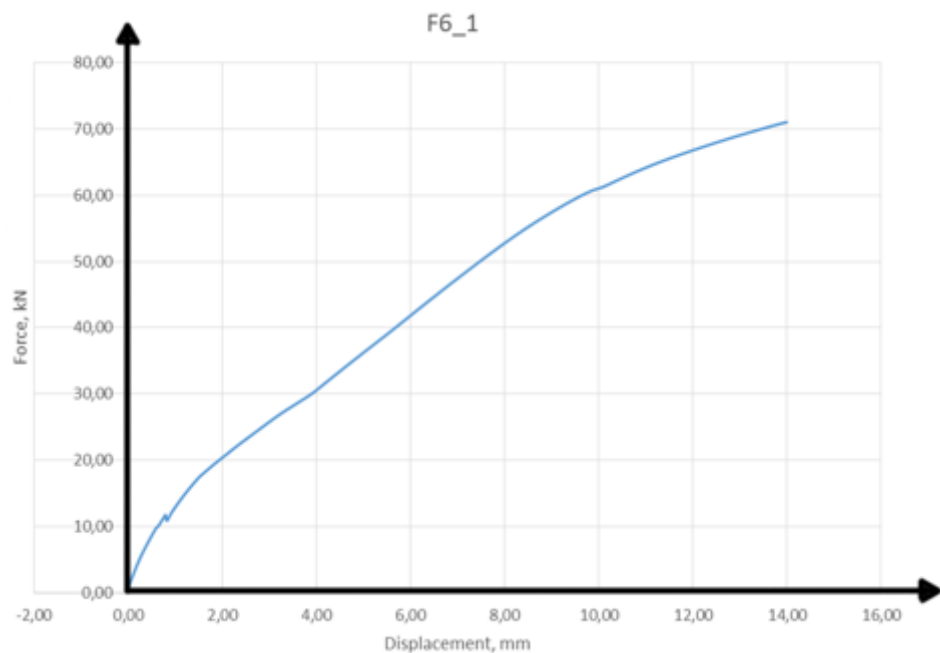


Figure 48. Load-displacement graph for the specimen F6_1 of *Giraldo (2018)*

However, it is important to note that *Giraldo (2018)* tests are far from perfect. The arrangement was made weaker than needed, allowing a permanent deformation to develop in the holding apparatus thus adding an additional displacement and load to the final result. Because plastic bent allowed for a bit (at least 2 mm) of free movement and required additional energy to reach failure. Therefore, possibly, increasing the failure force.

Nevertheless, keeping the speculation away, FE model seems to be an ideal version of *Giraldo (2018)* tests, due to the integrity of its load path and load application. The problem with verification of this statement is that material properties are hard to define, especially in case of HAZ.

Therefore, visually the model follows the clues of *Giraldo (2018)* specimen F6_1, but fails to produce a similar load-displacement graph. More tests and models are needed.

4 CONCLUSION

A modicum of success was achieved with this thesis. More has to be done to make a good simulation of a test arrangement presented in *Giraldo (2018)*, but the groundbreaking work has been done already.

Unfortunately, the results of the simulation compared by the load-displacement graph to the test results of the specimen F6_1 of *Giraldo (2018)* do not reach convergence. However, it is the result of a composite problem of parameter definition and accuracy of execution of tests.

5 RECOMMENDATIONS AND FUTURE WORK

In conclusion of the monumental work done for this thesis (subjective perception of the author), a few recommendations are given - divided into modelling and testing segments.

5.1.1 On the modelling side

In order to improve FE model, better data for material properties definition is dearly needed. Prior tensile tests of parent material and technical delivery notes on parent and filler materials are essential for a successful

simulation. Also, additional tests and multiple HAZ material models are required (in both stress-strain and formation due to heat treatment), so justice can be served to such an intriguing concept and further mysteries uncovered.

5.1.2 On the testing side

Tests need to be organized with clearly predefined goals and procedures. A predetermined test program and analysis algorithm are important, as well as results that are predictable and well documented. The next step in this direction is the upcoming thesis by Lev Antimonik in *Antimonik (2019)*.

More tests in for each identical specimen should be performed (at least three), in order to provide a better selection for statistical support of decision-making.

5.1.3 Organizational suggestions

As for future Bachelor theses, it will be exciting to intertwine mathematical modelling and testing. For example, by commissioning a pair of students to work alongside each other, cracking the same riddle from two fronts - supporting each other and the research.

Overall, plenty of good work needs to be done in order to bring high strength steels into the mainstream of structural engineering.

REFERENCES

Abebe, E. (2016). *Effect of heat input on the mechanical properties of high strength steel half V-welded joints*. Bachelor's thesis. Degree Programme in Construction Engineering. HAMK University of Applied Sciences.

Antimonik, L. (2019). *Test arrangement for high strength steel welded T-joints tensile tests*. Bachelor's thesis. Degree Programme in Construction Engineering. HAMK University of Applied Sciences. (Unfinished at the time of completion of this Bachelor's thesis).

Digital Engineering. *Difference between plane stress and plane strain formulations of shells*. Retrieved on 12th of March 2019. From: <https://www.digitalengineering247.com/article/simplifying-fea-models-plane-stress-and-plane-strain/>

ESAB. *OK ARISTOD 69 Product Information*. Retrieved on 12th of March 2019. From: <https://www.esab.co.uk/gb/en/products/welding-consumables/mig-mag-wires-gmaw/low-alloy-wires/ok-aristorod-69.cfm>

Garifullin, M. et al (2017). *Initial in-plane rotational stiffness of welded RHS T joints with axial force in plane member*. An article. Journal of Constructional Steel Research. Elsevier Publishing Ltd.

Giraldo, J. (2018). *Effect of heat input on the mechanical properties of high strength steel T-joints*. Bachelor's thesis. Degree Programme in Construction Engineering. HAMK University of Applied Sciences.

Grecevci, B. (2016). *Effect of heat input on the mechanical properties of high strength steel butt-weld joints*. Bachelor's thesis. Degree Programme in Construction Engineering. HAMK University of Applied Sciences.

Harari, Y. (2011). *Sapiens: A Brief History of Humankind*. Vintage/Penguin Random House publishing.

Jaspart, J. and Weynard K. (2016). *Design of Joints in Steel and Composite Structures*. ECCS Eurocode Design Manuals. Ernst & Sohn Publishing.

LS-Dyna online support/encyclopaedia. Retrieved on 12th of March 2019. From: <https://www.dynasupport.com/>

LS-PrePost online documentation. Retrieved on 12th of March 2019. From: <http://www.lstc.com/lsp/lspp/index.shtml>

LSTC (2012). *LS-Dyna User's Manual Volume 1 (for version 971 R6.1.0)*. Livermore Software Technology Corporation (LSTC).

LSTC (2012). *LS-Dyna User's Manual Volume 2 (for version 971 R6.1.0)*. Livermore Software Technology Corporation (LSTC).

Martin, G. (1996). *A Game of Thrones*. Voyager Books.

Nguyen, V. (2018). *Effect of heat input on the mechanical properties of butt-welded steel joints*. Bachelor's thesis. Degree Programme in Construction Engineering. HAMK University of Applied Sciences.

Perelmuter, A. and Slivker, V. (2003). *Numerical Structural Analysis*. Springer publishing.

Plutarch. *Comparative Lives*. Penguin Random House

RFCS of European Commission (2016). *Rules on high strength steel (RUOSTE)*. Research Report. Research Fund for Coal and Steel.

SFS-EN 1990 (2002). *Basis of structural design*. SFS.

SFS-EN 1993-1-1 (2005). *Design of buildings*. SFS.

SFS-EN 1993-1-8 (2005). *Design of joints in steel structures*. SFS.

SFS-EN 1993-1-12 (2007). *Additional rules for the extension of EN 1993 up to steel grades of S700*. SFS.

SSAB. *Techsupport #64: Static strength in joints of Strenx grades*. SSAB Corporation.

SSAB. *Welding of Strenx*. SSAB Corporation.

SSAB (2008). *Data Sheet for Strenx 700MC*. SSAB Corporation.

The Wire (2002 – 2008). HBO. TV series.

VarmintAI, *Notes and stories of LS-Dyna user*. Retrieved on 12th of March 2019. From:

<http://www.varmintal.com/aengr.htm#Mats-for-LS-DYNA>

INTERVIEWS

Havula, J and Ma, Z. (2018). First, is the Head of HAMK Tech and second is a lecturer in HAMK University of Applied Science. Interview on *08th of November 2018*.

Presenting intermediate results.

Havula, J and Ma, Z. (2019). First, is the Head of HAMK Tech and second is a lecturer in HAMK University of Applied Science. Interview on *14th of February 2019*.

Presenting thesis draft and narrative structure, as well as final model results.

Ma, Z. (2018). Lecturer in HAMK University of Applied Sciences. Interview on *01st of May 2018*.

Discussing principles of work and calculations of LS-Dyna.

Ma, Z. (2018). Lecturer in HAMK University of Applied Science. Interview on *04th of September 2018*.

Discussing updates to the model.

Ma, Z. (2018). Lecturer in HAMK University of Applied Science. Interview on *20th of November 2018*.

Presenting further intermediate results.

Saastamoinen, A. (2018). Lecturer in HAMK University of Applied Sciences. Interview on *30th of April 2018*.

Discussing properties of HAZ and their prediction.

Modelling order

"Engineer's curse is to submit to the whims of curiosity."

The following is a proposed modelling order:

1. Collect the data from tests
2. Define geometry of the model
3. Choose element type and size
4. Divide model into parts
5. Define material model and material properties
6. Assign material properties to a relevant part
7. Define load and support conditions
8. Define termination time for the simulation
9. Run the model
10. Extract and analyse the results

Problem of elongation measurement

"It is never too late to panic" – Ciaphas Cain, Hero of the Imperium

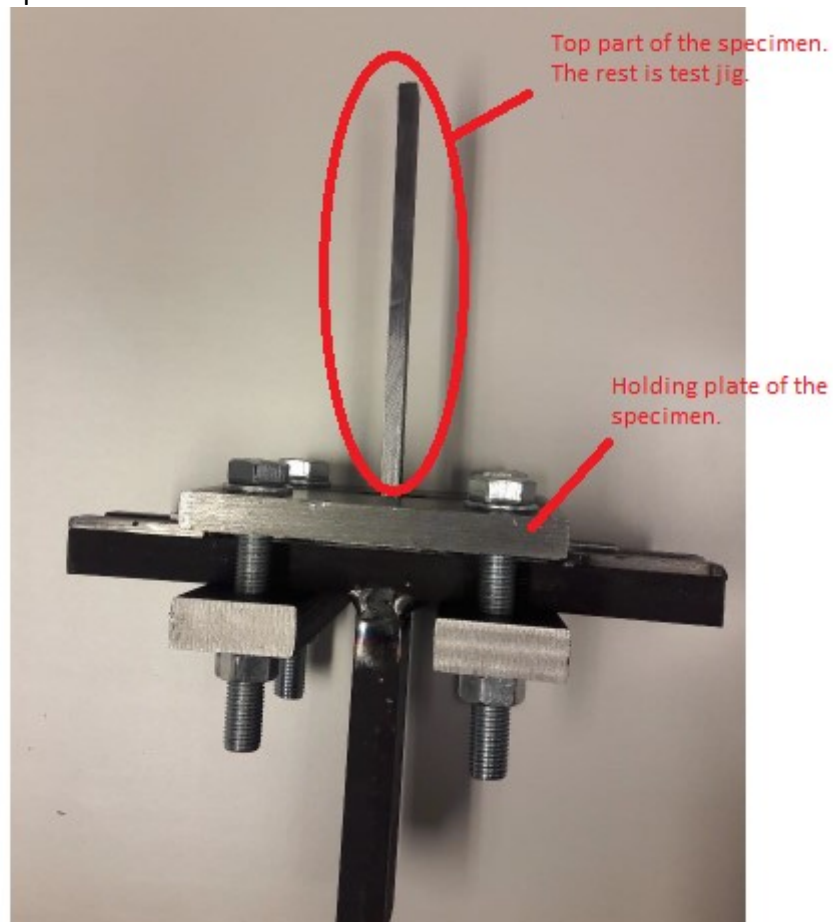
Now to address general problem of all those tests specimens. The problem of measurement of elongation. As you can notice from summaries of failures of specimens from *Giraldo (2018)* - elongation varies even in similar weld geometries. Elongation of the specimen is important, because strain is derived from it and strain is the cornerstone part of the function describing deformation of the element in FEA. But we will cover definition of material and its influence in further sections.

Here are a few causes of uncertainties in estimation of elongation:

I. Plastically deformed test jig

The most obvious perpetrator of the differences in deflection is the testing jig.

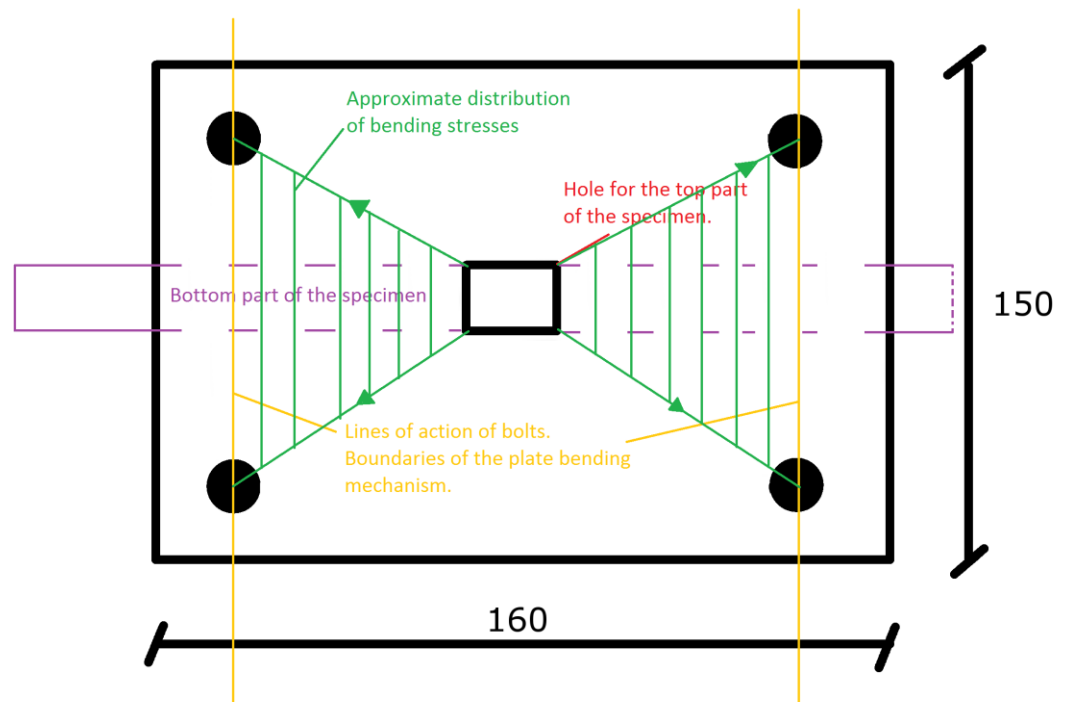
Here is a picture of it before the first test:



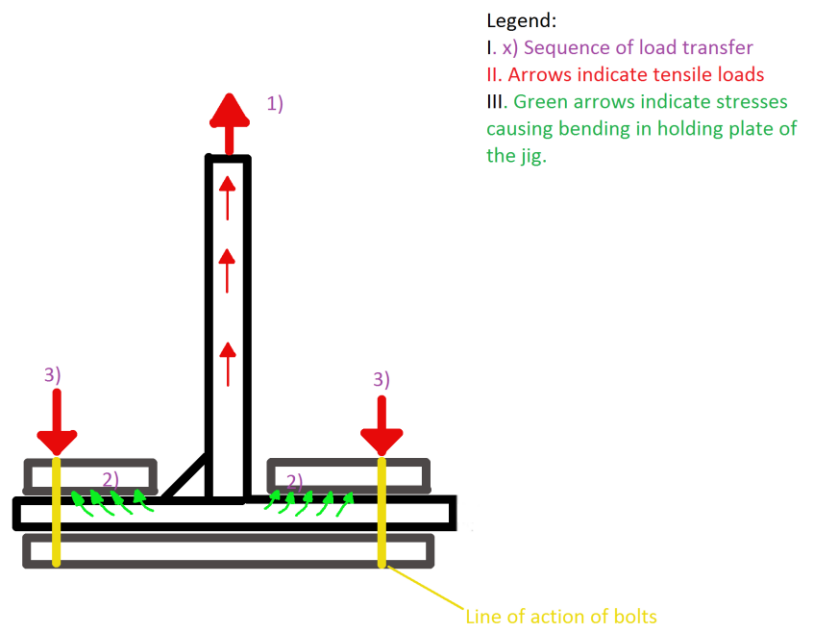
As you can see in the picture above, the testing jig is a massive structure compared to the specimen itself. Its massive design is set to completely restrain the specimen and avoid any deformation in the bottom part of the specimen. Thus, the bending of the bottom part of the specimen is not adding to the ultimate resistance of the joint (see chapter on the restraints design).

Here is a schematic drawing of the holding plate (with approximate dimensioning):

Appendix 2 (page 2)

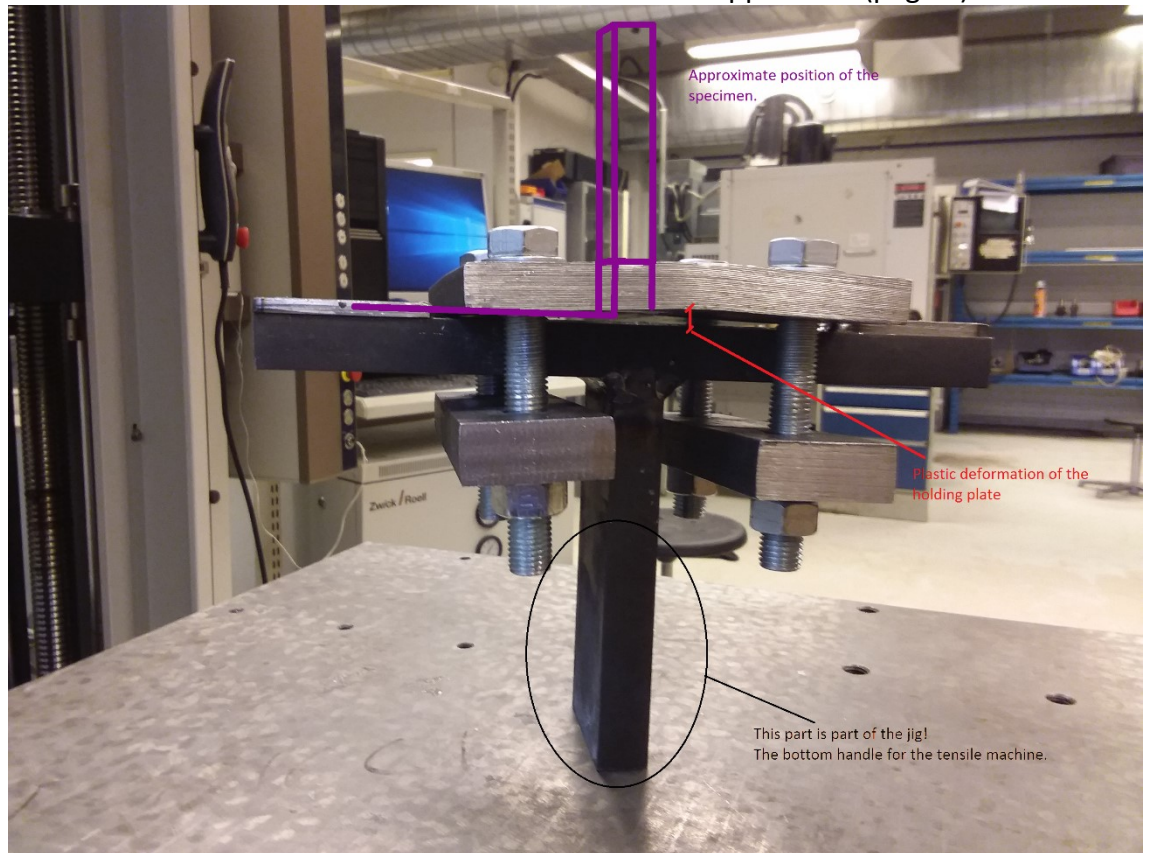


In addition, here is a schematic drawing of the bending mechanism and the load path of the holding plate of the jig:



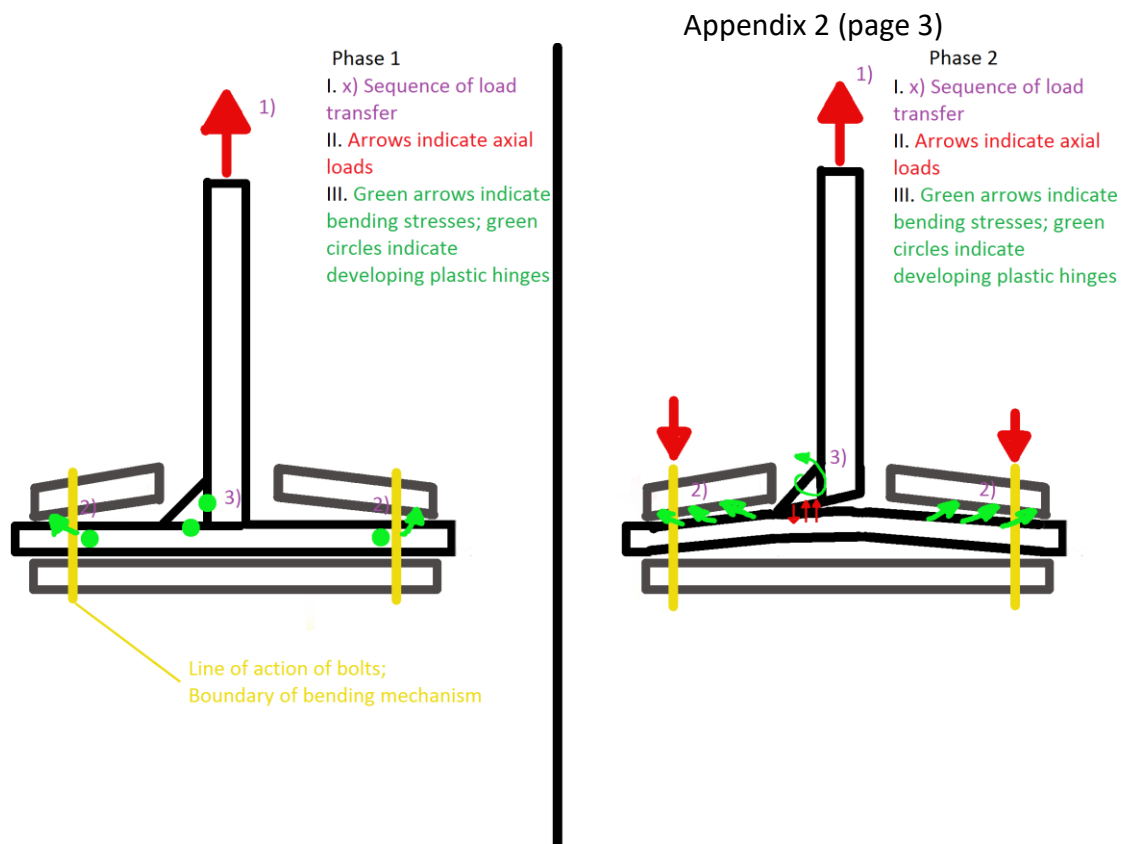
This was the planned load distribution in the top part of the jig. However, nothing is perfect. Here is a picture of the testing jig before final series of tests (including F6_1):

Appendix 2 (page 3)



The above photo is taken before the test specimen was put into the jig (approximate position of the specimen is shown in purple for convenience). So that plastic deflection of the holding plate is easier to notice. This bend affects both elongation measurement and boundary conditions. Thus being the source of both geometrical and material uncertainties.

Such a deformation causes the load transfer mechanism to become a two-phased one. Here is a sketch (note over exaggerated deformations):



A range of motion allowed to the specimen by plastic bent in the holding plate, creates conditions for the development of plastic hinges in the bottom part of the specimen, increasing necessary energy to achieve a collapse of the weld and thus increasing the force necessary to achieve collapse of the specimen. Also, two-phase behaviour is extremely hard to model, especially when weld properties are concerned (see section on material properties).

This mode of behavior was verified by one of the many FE tests in LS-Dyna. It was possible because of approximate measurements of the plastic bent made. Comparison tests using specimen F6_1 data and varied support conditions were performed. Specimen F6_1 was used since it was the last specimen tested in *Giraldo (2018)*.

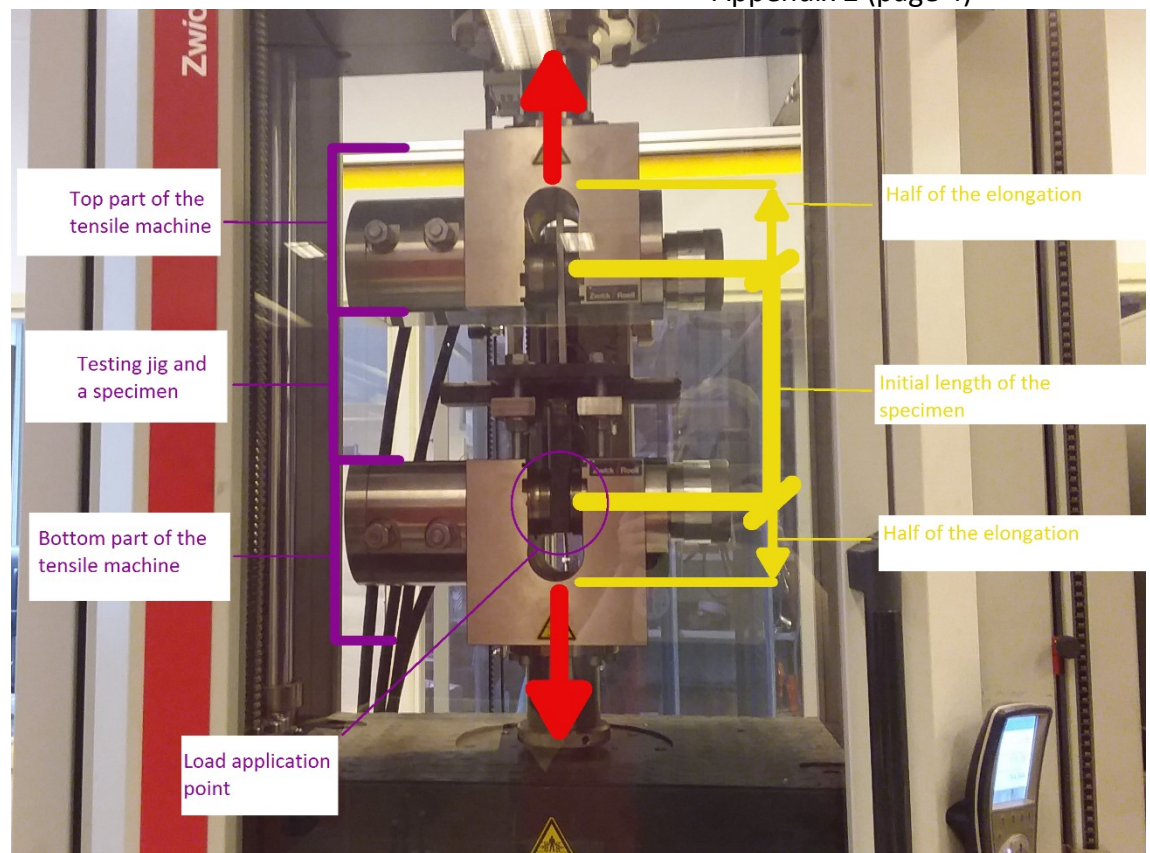
Even though permanent bent is about 4 mm, the effect on the model behaviour is profound.

It is no surprise that such problematic test arrangement was sent for further development. For more details see *Antimonik (2019)*.

II. Measurement by tensile machine only (length of the movement done by the claw)

The second cause of uncertainty is the measurement performed by the tensile machine itself. The machine measures its total vertical movement and that is about it. Here is a picture illustrating this principle:

Appendix 2 (page 4)



In normal tensile tests the provided level of precision is enough to derive strain of the material. However, in more complex test arrangements (as in *Giraldo (2018)*) those values are impossible to use in determination of strain of the material (in our case of HAZ, considering it is the failure zone). This brings us to the next point.

III. Lack of strain gauges (Note that placing it on such a small weld is practically impossible).

The third cause of uncertainties in measurement of elongation is impossibility to use strain gauges.

Strain gauges is a small measuring device, which is glued to a specimen. It measures the elongation of a segment of a structure along one of the axes. Normally, it would have been applied to the centre of a tensile test specimen, but in our case we have no location to apply it - because due to jig and test planning imperfections - strain does not go along a singular axis. In addition, it requires a significant effort to apply strain gauge and then analyse information obtained.

Methodology of engineering to true conversion

In short, the methodology looks as follows:

$$\text{True strain} = \ln(1 + \text{engineering strain})$$

$$\text{True stress} = (\text{engineering stress}) * \exp(\text{true strain}) = (\text{engineering stress}) * (1 + \text{engineering strain})$$

$$\text{Effective plastic strain (input value)} = \text{total true strain} - \text{true stress}/E$$

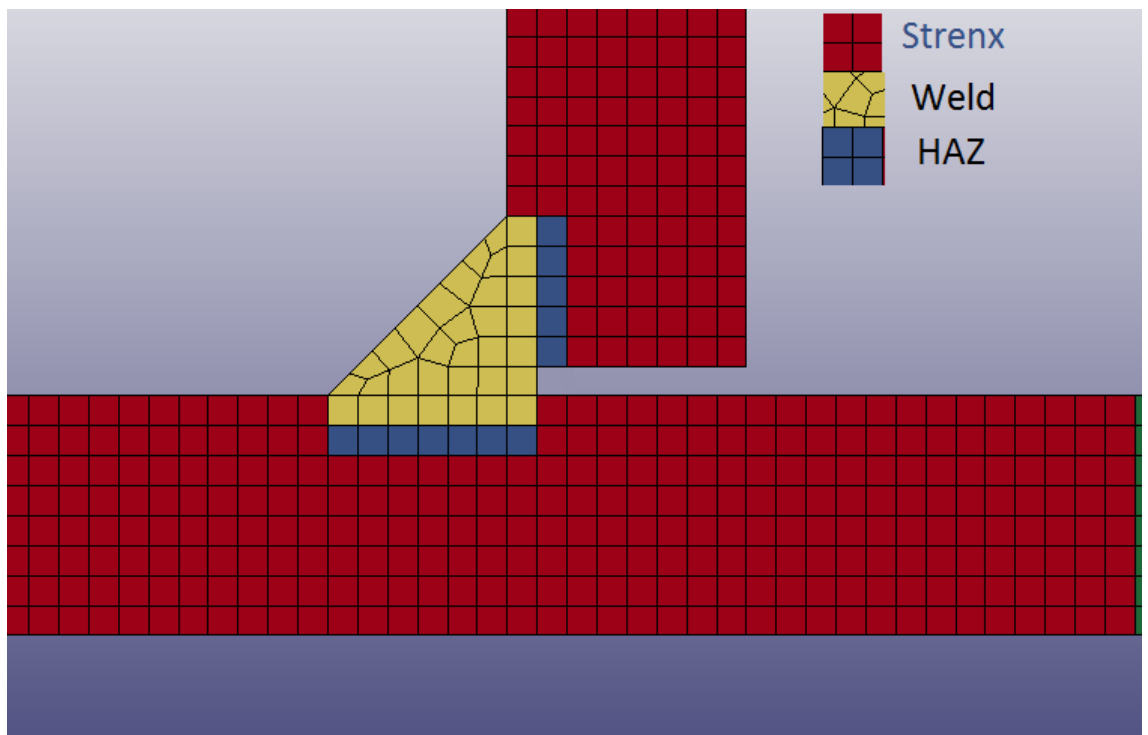
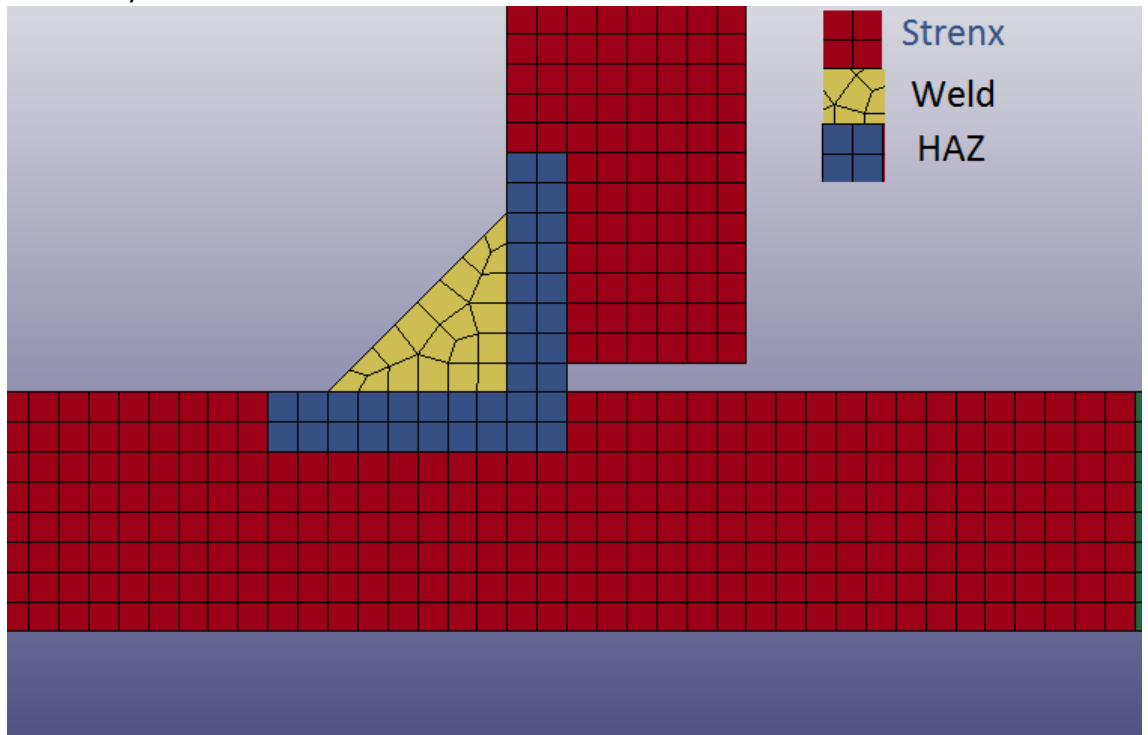
Where E is modulus of elasticity.

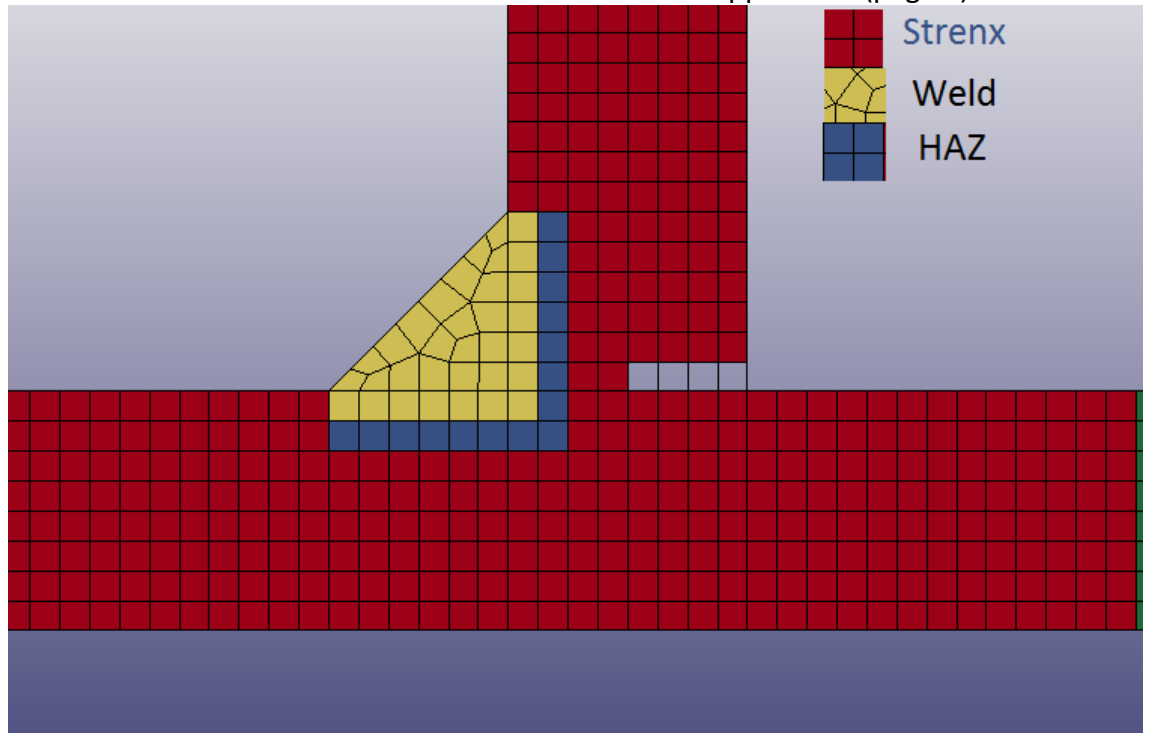
$$\text{Effective plastic stress (input value)} = \text{True stress at the point of effective plastic strain}$$

More information can be found here:

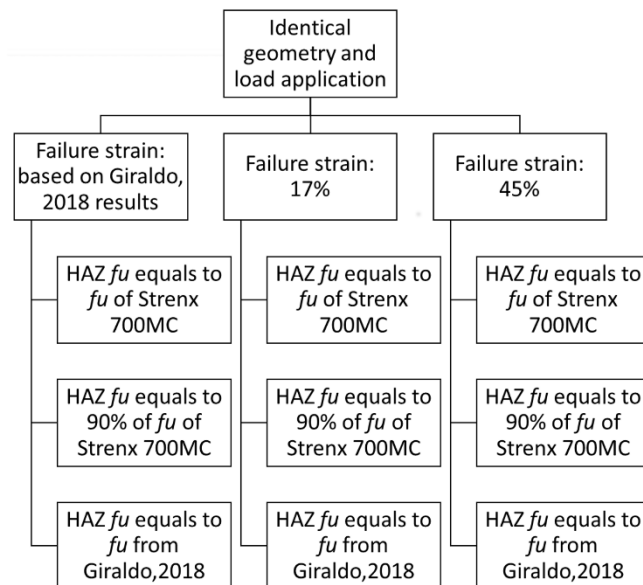
<https://www.dynasupport.com/howtos/material/from-engineering-to-true-strain-true-stress> (accessed on 11th of March 2019)

Other options for weld/HAZ balance





In addition, a suggestion for the determination of material properties:



MAT024 Input

Keyword Input Form

NewID

Use *Parameter Comment (Subsys: 1 F6F_2D_311018_ELF0RM12.k)

*MAT_PIECEWISE_LINEAR_PLASTICITY_(TITLE) (024) (3)

TITLE
Strenx 700

1	<u>MID</u>	<u>RO</u>	<u>E</u>	<u>PR</u>	<u>SIGY</u>	<u>ETAN</u>	<u>FAIL</u>	<u>TDEL</u>
	1	7.800e-06	200.00000	0.3000000	0.7024500	0.0	0.1535000	0.0
2	<u>C</u>	<u>P</u>	<u>LCSS</u>	<u>LCSR</u>	<u>VP</u>			
	0.0	0.0	0	0	0.0			
3	<u>EPS1</u>	<u>EPS2</u>	<u>EPS3</u>	<u>EPS4</u>	<u>EPS5</u>	<u>EPS6</u>	<u>EPS7</u>	<u>EPS8</u>
	0.0	0.0381000	0.0781000	0.1165000	0.1535000	0.0	0.0	0.0
4	<u>ES1</u>	<u>ES2</u>	<u>ES3</u>	<u>ES4</u>	<u>ES5</u>	<u>ES6</u>	<u>ES7</u>	<u>ES8</u>
	0.7024500	0.8340000	0.9331000	0.9696500	1.0060000	0.0	0.0	0.0

Total Card: 3 Smallest ID: 1 Largest ID: 3 Total deleted card: 0

Before getting to the details, it is important to keep the consistency of units in LS-Dyna input. Software itself does not check the consistency. Unit consistency of the output depends on the unit consistency of the input.

For example, in this thesis GMAT system was used (kg, mm, ms, kN, GPa, kN*mm).

Row 1:

From left to right. Material id in the model, for identification in definition of *Part properties. Density of the material. Modulus of elasticity. Poisson ratio. True value of yield stress. Tangent modulus. Effective plastic failure strain, value of true strain at which the element is deleted. Minimum time step size for automatic element deletion.

Row 2:

First two parameters relate to strain rate, which we do not need since our simulation happens at relatively low speed. Two options for predefined curves (LS-Dyna Manual volume 2 has more information). Formulation of rate effects.

Row 3:

Point by point definition of Effective Plastic Strain up to Effective Plastic Failure Strain (EPFS). Correlates vertically with the next row.

Row 4:

Point by point definition of Effective Stress, correlating to Effective Plastic Strain.

About heat input

As a side note, one run welds like F6_1 do not conform to recommendations made by SSAB in their welding guide for Stenx.

FIGURE 19 Maximum recommended heat input (Q) for Stenx 700.

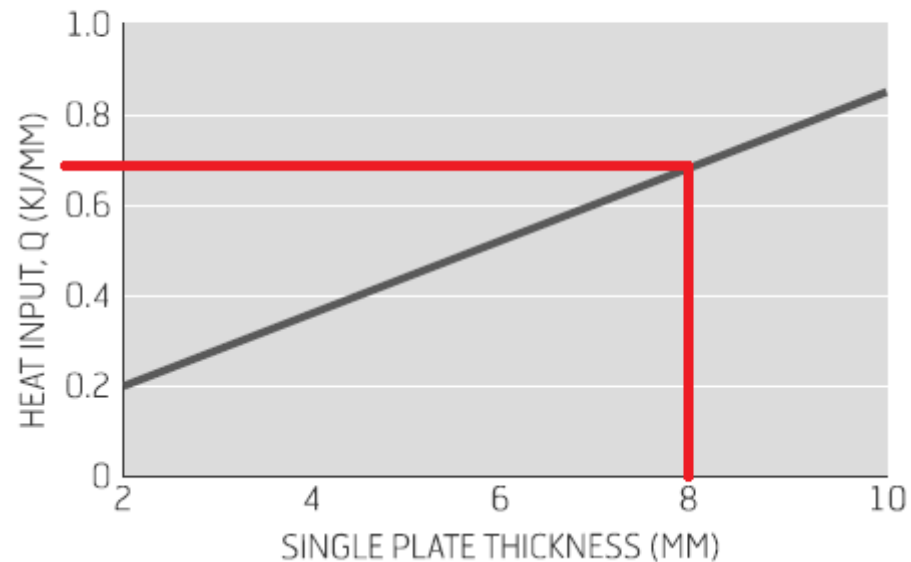


Figure taken from SSAB Welding Guide for Stenx

Table 1. S700 heat input

Sample name ¹⁾	weld length (mm)	First run		Second run		Third run	
		Welding speed (mm/s)	Heat input (kJ/mm)	Welding speed (mm/s)	Heat input (kJ/mm)	Welding speed (mm/s)	Heat input (kJ/mm)
S700-1R	200	1.87	1.37	-	-	-	-
S700-2R	200	2.53	0.71	2.85	0.87	-	-
S700-3R	200	2.081	0.82	4.347	0.49	4.34	0.51

¹⁾ Sample name: [Steel grade]-[Number of weld run(R)]

From Nguyen (2018)

Table 4 Heat input results, obtained with the ArcData catcher.

Specimen's name	Run number	Welding time (s)	Welding current (A)	Wire voltage (V)	Welding speed mm/s	Calculated heat input (kJ/mm)
B8 (Butt weld 8mm)	1	127	209.70	21.80	3.15	1.16
F6 (fillet weld 16mm)	1	97	274.9	29.3	4.12	1.56
F10	1	78	280	29	5.13	1.27
F10	2	64	258.4	29.5	6.25	0.97
F10	3	69	272.9	29	5.8	1.1
F12	1	87	283	29.2	4.6	1.44
F12	2	77	269	29.5	5.19	1.06
F12	3	22.3 (1)	283.3	29	5.38 (1)	1.18

(1) Wire ran out during welding. Only 120mm from the total 400 mm of the specimen's length was welded.

From Giraldo (2018)

*weld size of F6 is noted incorrectly - it is 6mm, not 16mm.

Appendix 6 (page 2)

The recommended heat input is about 0.7 kJ/mm while the results are 1.37 kJ/mm and 1.56 kJ/mm. This means that deviation from recommended values are 95% and 122% respectively. Such a deviation of heat input partially explains low ultimate tensile stress of HAZ in regards to the parent material. Thus making the third option based on test results more feasible than educated guess of 90% of f_u of Strenx 700MC.

Some sources for self-tutelage in LS-Dyna

“There is much to learn. Much to discuss.” – Optio Bologna

Here is a list of some sources used in creating this thesis, which can help with modeling:

- <https://www.dynasupport.com/> - official support website
- <http://www.varminal.com/aengr.htm#Mats-for-LS-DYNA>
interesting information on material modelling
- <http://www.lstc.com/lsp/index.shtml> - official tutorials etc for LS-PrePost
- https://www.youtube.com/watch?v=3a_T7Hh19gQ& simple introduction to LS-PrePost environment

As well as, official LS-Dyna Manuals (Volume 1 and Volume 2)